

Permutation Relations of Yangian Invariants

Peizhi Du, Gang Chen¹, and Yeuk-Kwan E. Cheung²

*Department of Physics, Nanjing University
22 Hankou Road, Nanjing 210093, P. R. China*

E-mail: gang.chern@gmail.com, cheung@nju.edu.cn

ABSTRACT: We find a permutation relation among Yangian Invariants – two Yangian Invariants with adjacent external lines exchanged are related by a simple kinematic factor. This relation is shown to be equivalent to U(1) decoupling and Bern-Carrasco-Johansson (BCJ) relation at the level of maximal helicity violating (MHV) amplitudes. Together with the newly found permutation relation and using unitarity cuts to remove ambiguity in the definition of loop momenta of cut amplitudes due to the nonplanar legs, we propose a systematic way of reconstructing the the integrands of nonplanar MHV amplitudes up to a rational function which vanishes under all possible unitarity cuts. This method when applied to planar diagrams reproduces results from the single cut method. As explicit examples the construction of one-loop double-trace MHV amplitudes of 4- and 5-point interactions are presented using on-shell diagrams. The kinematic factors and the resultant planar diagrams are carefully dealt with using the unitarity cut condition. The first next-to-MHV amplitudes are addressed using generalized unitarity cuts. Their leading singularities can be identified as residues of the Grassmanian integral. This example also serve to demonstrate the power of the newly found relation of Yangian Invariants.

KEYWORDS: Permutation relation, Yangian Invariants, N=4 super Yang-Mills, Non-planar amplitudes, Unitarity cuts, BCFW

¹Corresponding author

²Corresponding author

Contents

1	Introduction	2
2	A permutation relation among Yangian Invariants in on-shell diagrams	4
2.1	Permutation relation of box in bipartite diagrams	4
2.2	Kinematic factors	7
2.3	Permutation relations for NMHV amplitudes—a twin-box connected by a BCFW bridge	11
3	Unitarity cuts and generalized unitarity cuts	14
3.1	Unitarity cut	15
3.2	Generalized unitarity cuts	18
4	MHV Loop Amplitudes	20
4.1	MHV planar amplitudes and unitarity cuts	21
4.2	MHV nonplanar amplitudes and unitarity cuts	34
4.3	One-loop four-point MHV nonplanar amplitudes	38
4.4	One-loop five-point MHV nonplanar amplitudes	40
5	NMHV nonplanar amplitude from double unitarity cuts	42
6	Conclusion and Outlook	48
A	The momentum twistor space	51

1 Introduction

The recent progress in the computation of Yang-Mills scattering amplitudes has been exciting. At tree level, BCFW recursion relation [1–4] can be used to calculate n -point amplitudes efficiently. Unitarity cuts [5–7] and generalized unitarity cuts [8–14] combined with BCFW for the rational terms work well at loop level [15–20]. All loop integrands [21–24] for $\mathcal{N} = 4$ super Yang-Mills (SYM) planar amplitudes can be obtained recursively in principle. On the other hand there is much progress on gluon amplitude computation at strong coupling [25, 26] via the celebrated AdS/CFT correspondence.

Besides the progress on calculations interesting and useful relations among color-ordered partial amplitudes have been uncovered. A relation of such kind was proposed by Bern, Carrasco and Johansson [27], the BCJ relation. Together with the KK relation proposed earlier by Kleiss and Kuijf [28], these two relations have since then been widely used to simplify calculations at tree level [29–34].

Lately Arkani-Hamed et al [35] proposed using positive Grassmannian to study $\mathcal{N} = 4$ super Yang-Mills along with the constructions of the bipartite ribbon on-shell diagrams [36]—in which all internal legs are *on shell*—for planar Yang-Mills interactions. In such a construction each on-shell bipartite diagram is automatically gauge invariant; and a direct relationship between planar amplitudes in $\mathcal{N} = 4$ super Yang-Mills (SYM) and the positive Grassmannian structures is presented. Furthermore they also prescribe a permutation rule for characterizing on-shell diagrams of tree level amplitudes as well as the leading singularities [37, 38] in planar loop-level amplitudes. Specifically each on-shell diagram corresponds to a Yangian invariant [39, 40]; and the scattering amplitudes can be obtained by summing over the underlying Yangian Invariants. All can be done in either the momentum space or the momentum twistor space [41–43].

On-shell bipartite diagrams fall into equivalence classes under square moves and mergers. Such equivalence operations leave the corresponding Yangian Invariants unchanged. However if we only require the corresponding Grassmannian geometry unchanged, by intuition, there should be new generators of equivalence operations. In this paper, we will discuss a class of such operations generated by a black & white (B&W) square—which for the rest of the paper will be called a “basic box”—leading to permutation relations in the on-shell diagrams. These, in turn, induce relations among Yangian invariants.

Another motivation for this work is to present a systematic method to construct

the local integrands [22, 44] of Yang-Mills scattering amplitudes from unitarity cuts for planar diagrams. Under each unitarity cut, the integrand of the amplitude is well-defined and can be obtained by gluing tree-level amplitudes. According to the on-shell diagrams of the tree-level amplitudes, we can directly remove the unitarity cut constraints in the frame of on-shell diagram. Then for each unitarity cut we obtain a simple form of the integrand up to a rational function which will vanish on the unitary cut. After introducing a proper operation to combine the integrands for all kinds of the unitarity cuts, we can get an integrand for an general amplitude up to a rational function which will vanish under all the unitarity cuts. According to the unitarity constructible condition for the amplitudes in super Yang-Mills theory [5, 6], the final ambiguity of the integrand can be fixed by setting the rational function to zero. Then we obtain the final form of the integrand for the amplitude. This method enjoys a direct extension to nonplanar diagrams when combined with the newly found on-shell permutation relations. In nonplanar diagrams¹ it is still possible to define an integrand up to rational functions which will vanish under all the unitarity cuts [45–49].

Unitarity cuts are deployed, in nonplanar diagrams, to remove the well-known ambiguity in loop momentum definition due to the nonplanar leg(s), as opposed to single cuts used by Arkani-Hamed et al [35] in the construction of planar amplitudes. A good definition of loop momentum under a unitarity cut in the nonplanar loop diagrams will be presented. The resulted diagrams after a unitarity cut of a given one loop nonplanar diagram (by which we mean one-loop double-trace amplitudes) can be transformed into the on-shell diagrams. Using our newly found on-shell permutation relation a nonplanar on-shell diagram could be subsequently converted to (a linear combinations of) planar diagrams with kinematic functions as coefficients. One then needs to sum up the resultant planar diagrams, from all possible unitarity cuts of a given nonplanar diagram, to obtain the total nonplanar amplitudes after unitarity cuts.

The final step of our construction is to use appropriate BCFW bridges to reconstruct the total on-shell diagrams for a given nonplanar diagram. All possible but inequivalent connections by BCFW bridges need to be taken into account. The most crucial step is the discovery of the permutation relation for bipartite on-shell diagrams that enable us to convert nonplanar on-shell sub-diagrams into planar ones, which, in turn, enable the straight forward application of the existing techniques developed for on-shell planar diagrams. This method works is well-adapted for higher loops; and we believe that it can be generalized to higher-loop nonplanar diagrams (work in progress).

¹By “nonplanar diagrams” we mean either the loop line twisted nonplanar diagrams or the higher loop multi-trace diagrams. This is because both cases are of same form in on-shell diagrams.

We shall show by explicit computations in Section 4 that the total on-shell diagrams constructed by unitarity cuts for MHV nonplanar one-loop amplitudes in $\mathcal{N} = 4$ super Yang-Mills give the correct local integrands. The total on-shell diagrams constructed for NMHV nonplanar one-loop amplitudes by generalized unitarity cuts reproduce the correct integrals [50], as presented in Section 5.

2 A permutation relation among Yangian Invariants in on-shell diagrams

In dealing with nonplanar amplitudes it is crucial that there be a relation to enable the transformation of nonplanar elements into planar ones. To our pleasant surprise there exists such a simple relation, represented pictorially in Fig. 1 below. A permuta-

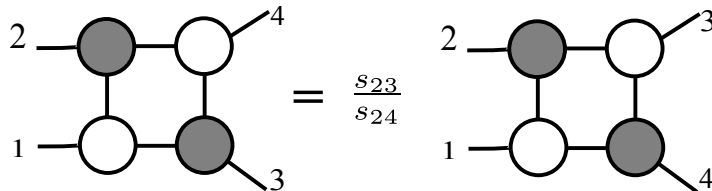


Figure 1. Yangian invariant relation in 4-point tree amplitude.

tion relation relating different Yangian invariants is completely analogous to the BCJ relation [27] for 4-point amplitude. We shall henceforth call such transformation *the permutation relation among Yangian invariants*.

In $\mathcal{N} = 4$ SYM the amplitudes can be constructed by unitary cuts or generalized unitary cuts. After cuts the loop amplitude is a combination of tree level amplitudes. As we want to transform the nonplanar amplitudes, after unitarity cut, into planar ones we need to know how the constituent tree amplitudes change under the permutations of legs. Since a permutation of legs is generated by a pairwise exchange of two consecutive legs we only need to know the transformations of the tree amplitudes under an exchange of two consecutive legs.

2.1 Permutation relation of box in bipartite diagrams

The set of rules governing the permutations of external legs for the bipartite on-shell diagrams have been introduced in [35]. Let us take, again, the box as an example: the 4-point tree amplitude has only one Yangian invariant. The corresponding permutation

is

$$\begin{pmatrix} 1 & 2 & 3 & 4 \\ 3 & 4 & 5 & 6 \end{pmatrix},$$

In a on-shell diagram of a tree-level amplitude a permutation is in one to one correspondence to a Yangian invariant, we can therefore use permutations to characterize Yangian invariants. Without loss of generality, we take the permuted external legs to be 3 and 4. It is then easy to see

$$Y_4^{(2)}(1, 2, 4, 3) = \frac{s_{23}}{s_{24}} Y_4^{(2)}(1, 2, 3, 4) \quad (2.1)$$

where $s_{ij} = (p_i + p_j)^2 = \langle i j \rangle [i j]$ and $Y_4^{(2)}(1, 2, 3, 4)$ is

$$Y_4^{(2)}(1, 2, 3, 4) = \frac{\delta^{2 \times 4}(\lambda \cdot \tilde{\eta}) \delta^{2 \times 2}(\lambda \cdot \tilde{\lambda})}{\langle 1 2 \rangle \langle 2 3 \rangle \langle 3 4 \rangle \langle 4 1 \rangle}. \quad (2.2)$$

This is exactly what has been depicted in Fig. 1 above.

We can now generalize to n-point MHV amplitudes. The corresponding permutation is

$$\begin{pmatrix} 1 & 2 & \cdots & i & \cdots & n-1 & n \\ 3 & 4 & \cdots & i+2 & \cdots & n+1 & n+2 \end{pmatrix}. \quad (2.3)$$

For MHV ($k=2$) amplitudes, $Y_n^{(2)}(1, 2, \dots, n)$ can be written explicitly,

$$Y_n^{(2)}(1, 2, 3, \dots, n-2, n-1, n) = \frac{\delta^{2 \times 4}(\lambda \cdot \tilde{\eta}) \delta^{2 \times 2}(\lambda \cdot \tilde{\lambda})}{\langle 1 2 \rangle \langle 2 3 \rangle \cdots \langle n-2 \ n-1 \rangle \langle n-1 \ n \rangle \langle n \ 1 \rangle} \quad (2.4)$$

We, for concreteness, take the permuting legs to be $n-1$ and n . As shown in Fig. 2, for MHV on-shell diagrams, it is always possible to connect a box directly to the pair of the permuting legs [35], evident from the expression $Y_n^{(2)} = Y_4^{(2)} \underbrace{\odot Y_3^{(1)} \odot \cdots \odot Y_3^{(1)}}_{n-4}$ together with the cyclic symmetry of the external legs. This box is nothing but the 4-point on-shell amplitude. Using (2.1), we obtain a permutation relation for any MHV amplitude

$$Y_n^{(2)}(1, 2, 3, \dots, n-2, n, n-1) = \frac{s_{\widehat{n-2, n-1}}}{s_{\widehat{n-2, n}}} Y_n^{(2)}(1, 2, 3, \dots, n-2, n-1, n). \quad (2.5)$$

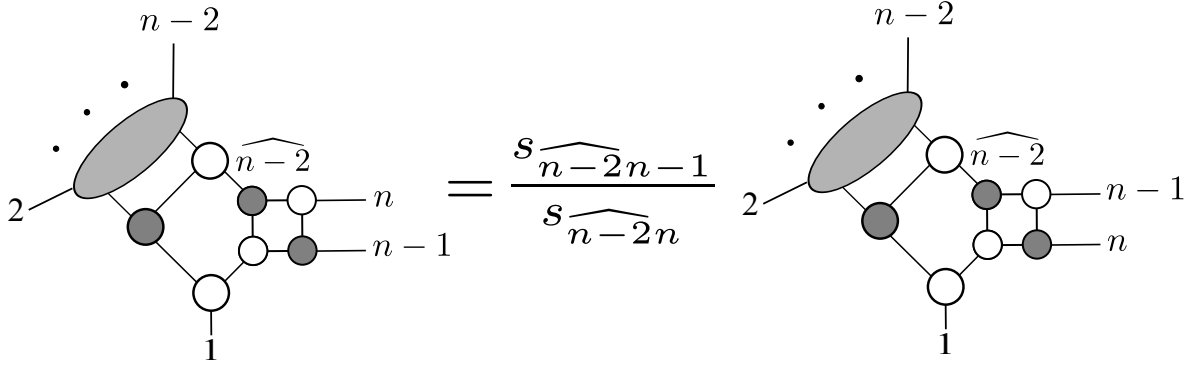


Figure 2. A Yangian invariant relation in 4-point tree amplitude, where ellipsis represent the process of adding “k-preserving inverse soft factors.”

The coefficient $\frac{s_{\widehat{n-2, n-1}}}{s_{\widehat{n-2, n}}}$ is obtained as followed (See Fig. 2.). Components other than the box, in a bipartite diagram, are just “k-preserving inverse soft factor $\odot Y_3^{(1)}$ ” [21]. Adding a factor $\odot Y_3^{(1)}$ does not change the spinors $\lambda_{\widehat{n-2}}$ and λ_1 ; and $\lambda_{\widehat{n-2}} = \lambda_{n-2}$ and $\lambda_1 = \lambda_1$. Altogether we get

$$\frac{s_{\widehat{n-2, n-1}}}{s_{\widehat{n-2, n}}} = \frac{\langle n-2 \ n-1 \rangle [\widehat{n-2} \ n-1]}{\langle n-2 \ n \rangle [\widehat{n-2} \ n]} = -\frac{\langle n-2 \ n-1 \rangle \langle 1 \ n \rangle}{\langle n-2 \ n \rangle \langle 1 \ n-1 \rangle}. \quad (2.6)$$

According to (2.5) and (2.6) the permutation relation we found is consistent with results for MHV amplitudes in the Parke-Taylor (2.4) form [51].

This new permutation relation holds, furthermore, for an analogous class of Yangian invariants in non-MHV amplitudes. To aid in the discovery we first establish a criterion suitable for this class of amplitudes. Firstly, we should define a modified BCFW-decomposition [35]. The on-shell diagram can be decomposed as taking apart a BCFW bridge from the diagram with a sub-diagram left. Then the permutation of the diagram σ can be decomposed as $(ij) \circ \sigma'$, where (ij) is the permutation of the BCFW bridge on i, j and σ' is the permutation of the left sub-diagram.

A BCFW-Bridge decomposition to a Box: Starting with a given permutation σ and picking two consecutive legs i and $i+1$, if $\sigma(i) \neq i \bmod n$ and $\sigma(i+1) \neq i+1 \bmod n$ and σ for the other legs is not identical to the identity modulus n (a “dressed” identity²), one can decompose σ as $(j_1 j_2) \circ \sigma'$, where $1 \leq j_1 < j_2 \leq n$ and $\sigma(j_1) < \sigma(j_2)$, with $j_1 \neq \{i, i+1\}$, and $j_2 \neq \{i, i+1\}$. The legs j_1 and j_2 are being separated only by the unpermuted legs or leg i , or $i+1$, keeping the order of $\sigma^{-1}(i), \sigma^{-1}(i+1)$ invariant.

²As an example, for $n = 6$ and $k = 3$, a dressed identity is $\{7, 8, 9, 4, 5, 6\}$.

One repeats the process until σ is an identity for all the legs except the legs $i, i + 1$ and $\sigma(i) \bmod n, \sigma(i + 1) \bmod n$. We denote the final permutation as $\bar{\sigma}$.

If, on the other hand,

$$\begin{aligned}\bar{\sigma}(i) &< \bar{\sigma}(i + 1) \\ \bar{\sigma}^{-1}(i) &< \bar{\sigma}^{-1}(i + 1),\end{aligned}\tag{2.7}$$

it is easy to see that the $\bar{\sigma}$ corresponds to a four point amplitude for legs $(i, i + 1, \sigma(i) \bmod n, \sigma(i + 1) \bmod n)$. Furthermore σ is obtained by putting BCFW bridges on $\bar{\sigma}$. Hence we conclude that the on-shell diagram corresponding to σ can have “a box” connecting directly to these two marked legs.

Moreover, in a BCFW-Bridge decomposition, we always keep the order of $\sigma^{-1}(i)$ and $\sigma^{-1}(i + 1)$. Then the condition (2.7) is equivalent to

$$\begin{aligned}\sigma(i) &< \sigma(i + 1) \\ \sigma^{-1}(i) &< \sigma^{-1}(i + 1),\end{aligned}\tag{2.8}$$

which is a convenient criterion on permutations to check whether a “box” can enjoy direct connection to a pair of adjacent legs in a on-shell bipartite diagram.

An application: In all MHV amplitudes, any two consecutive legs $\{i, i + 1\}$ are in “a box” due to $\sigma(i) < \sigma(i + 1)$ for the permutation σ of MHV amplitude (2.3). This observation agrees with [35]. For general Yangian invariants, with two consecutive legs $n - 1$ and n , if the condition (2.8) holds we have

$$Y_{\sigma_n}^{(k)}(1, 2, 3, \dots, n - 2, n, n - 1) = \frac{\widehat{S}_{n-2, n-1}}{\widehat{S}_{n-2, n}} Y_{\sigma_n}^{(k)}(1, 2, 3, \dots, n - 2, n - 1, n)\tag{2.9}$$

when permuting the pair of legs $n - 1$ and n , as shown in Fig. 3.

Conclusion: For planar bipartite on-shell diagrams, we can use the criterion (2.8) to justify if any two adjacent legs fall into a box.

2.2 Kinematic factors

Let us now turn our attention to the kinematic factors—the remaining obstacle in the construction of total integrands for nonplanar amplitudes. How to deal with the resultant planar diagrams as well as the concrete steps of reconstruction will be presented in Section 4 and 5. In this subsection, we also study the behavior of Yangian invariants

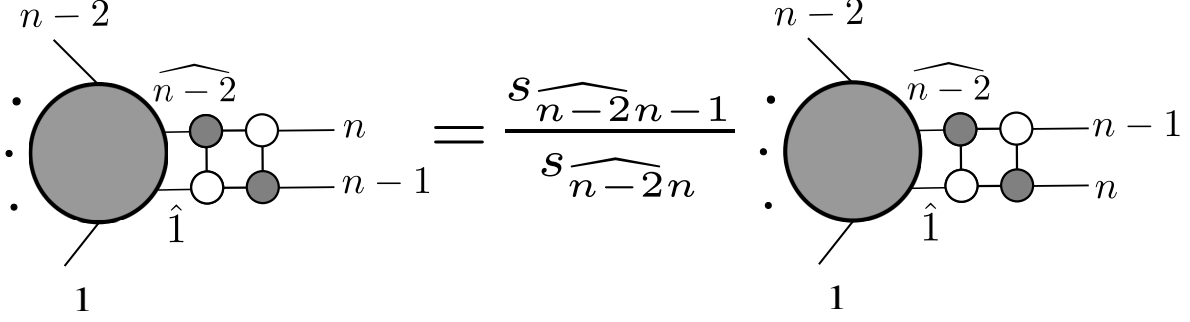
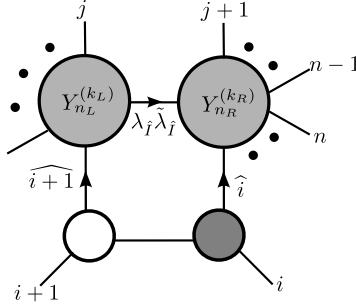


Figure 3. A Yangian invariant relation of a 4-point tree amplitude, with the dark circle denoting a general on-shell diagram.

Y_n^k and the corresponding Grassmannian cells, $(k \times n)$ -matrix C , under a permutation of two external legs. Each Grassmannian cell C is a point in the Grassmannian $G(k, n)$ which characterize the k -plane in the n -dimensional space.

To compute the kinematic factor $\frac{s_{\widehat{n-2n-1}}}{s_{\widehat{n-2n}}}$ we only need to determine the momenta of the two internal lines connecting to $Y_4^{(2)}$, which can be done recursively by BCFW method. We set a variable α to exhibit the momentum shift between $i+1$ and i ,



$\alpha \lambda_{i+1} \tilde{\lambda}_i$. Then the shifted momenta are

$$\lambda_{\widehat{i+1}} \tilde{\lambda}_{\widehat{i+1}} = \lambda_{i+1} (\tilde{\lambda}_{i+1} - \alpha \tilde{\lambda}_i)$$

and

$$\lambda_{\widehat{i}} \tilde{\lambda}_{\widehat{i}} = (\lambda_i + \alpha \lambda_{i+1}) \tilde{\lambda}_i.$$

The internal momentum connecting these two legs, $\lambda_I \tilde{\lambda}_I$, is determined by momentum conservation from the left (or right),

$$\lambda_I \tilde{\lambda}_I = \sum_k \lambda_k \tilde{\lambda}_k + \lambda_{\widehat{i+1}} \tilde{\lambda}_{\widehat{i+1}}$$

where the index k in the sum runs through all the external momenta on the left. The variable α can thus be solved by the condition $\lambda_I \tilde{\lambda}_I$ being on-shell

$$\left(\sum_k \lambda_k \tilde{\lambda}_k + \lambda_j \tilde{\lambda}_j + \alpha \lambda_i \tilde{\lambda}_j\right)^2 = 0. \quad (2.10)$$

The momenta $\lambda_I \tilde{\lambda}_I$ and $\lambda_j \tilde{\lambda}_j$ are fully determined by the spinors of the external momenta. And the Yangian invariant on the right is, in turn, determined.

We repeat the above operation until only a $Y_m^{(2)}$ (a MHV amplitude with $m < n$) is left. Using (2.5) and (2.6) we arrive at the desired kinematic factor $\frac{s_{\widehat{n-2, n-1}}}{s_{\widehat{n-2, n}}}$.

An example: An example is warranted here. In $Y_{\sigma_0 6}^{(2)}(1, 2, 3, 4, 5, 6)$, where σ_0 is taken to be $\{4, 5, 6, 8, 7, 9\}$, we take 5 and 6 to be the permuting legs. According to (2.8), such a Yangian invariant can have a “box” connecting to legs 5 and 6 directly as shown in Fig. 4, According to (2.9) we get

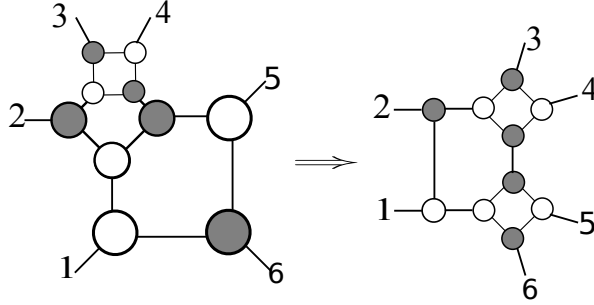


Figure 4. Transforming to an on-shell diagram with box connecting legs 5, 6 directly.

$$Y_{\sigma_0 6}^{(3)}(1, 2, 3, 4, 6, 5) = \frac{s_{\hat{4}5}}{s_{\hat{4}6}} Y_{\sigma_0 6}^{(3)}(1, 2, 3, 4, 5, 6). \quad (2.11)$$

The kinematic factor can hence be read off directly

$$\frac{s_{\hat{4}5}}{s_{\hat{4}6}} = -\frac{\langle \hat{4} 5 \rangle \langle 1 6 \rangle}{\langle \hat{4} 6 \rangle \langle 1 5 \rangle} \quad (2.12)$$

with $\lambda_{\hat{4}}$ being solved by (2.10)

$$\lambda_{\hat{4}} = (p_2 + p_3 + p_4) | \tilde{\lambda}_2] .$$

According to the arguments in [35] each on-shell diagram or Yangian invariant is associated with a differential form

$$d\Omega \delta(C \cdot \vec{\eta}) \delta(C \cdot \vec{\lambda}) \delta(\vec{\lambda} \cdot C^\perp), \quad (2.13)$$

where $d\Omega$ is the Grassmannian integration measure and C^\perp is orthogonal to C . The C can be taken as the matrix associated with the linear constraints $\delta(C \cdot \vec{\eta})$, $\delta(C \cdot \vec{\lambda})$, $\delta(\vec{\lambda} \cdot C)$ for the external spinors $\vec{\lambda}$, $\vec{\lambda}$, $\vec{\eta}$. The Grassmannian cell for a MHV amplitude is always

$$C = \begin{pmatrix} \lambda_1^1 & \lambda_2^1 & \cdots & \lambda_i^1 & \lambda_{i+1}^1 & \cdots & \lambda_{n-1}^1 & \lambda_n^1 \\ \lambda_1^2 & \lambda_2^2 & \cdots & \lambda_i^2 & \lambda_{i+1}^2 & \cdots & \lambda_{n-1}^2 & \lambda_n^2 \end{pmatrix}.$$

A permutation of two external lines does not change any of the linear constraints in (2.13). The Grassmannian cell is thus not affected by permutations when we fix the vector of external spinors. In fact this rule can be generalized to any on-shell diagrams in tree-level amplitudes. Any permutation of two external legs attached to a box does not affect the Grassmannian cell for a given vector of external spinors. This is easy to prove. Without lose of generality we take the permuted legs $n - 1$ and n . According to a BCFW decomposition to a box, the C matrix of an on-shell diagrams can be generalized by performing BCFW bridge on the C_0 matrix corresponding to $\bar{\sigma}$. The rows of C_0 are denoted by the i_w 's which satisfy $\bar{\sigma}(i_w) = i_w + n$, $\bar{\sigma}(n - 1) - n$ and $\bar{\sigma}(n) - n$. For the tree level on-shell diagrams the δ -functions are just enough to fix the parameters α_I 's. Hence the total number of BCFW bridge acting on a box is $2n - 8$; we obtain

$$C = C_0 \mathcal{B}(i_5, j_5; \alpha_5) \cdot \mathcal{B}(i_6, j_6; \alpha_6) \cdots \mathcal{B}(i_I, j_I; \alpha_I) \cdots \mathcal{B}(i_{2n-4}, j_{2n-4}; \alpha_{2n-4}), \quad (2.14)$$

where

$$\mathcal{B}(i_I, j_I; \alpha_I) = \begin{matrix} & & & & & & j_I & & \\ & & & & & & & & \\ & & & & & & & & \\ & & & & & & & & \\ i_I & \begin{pmatrix} 1 & 0 & \cdots & 0 & \cdots & 0 & \cdots & 0 \\ 0 & 1 & \cdots & 0 & \cdots & 0 & \cdots & 0 \\ \vdots & \vdots & \ddots & 0 & \cdots & 0 & \cdots & 0 \\ 0 & 0 & 0 & 1 & \cdots & \alpha_I & \cdots & 0 \\ \vdots & \vdots & \vdots & \vdots & \ddots & 0 & \cdots & 0 \\ 0 & 0 & 0 & 0 & 0 & 1 & \cdots & 0 \\ \vdots & \vdots & \vdots & \vdots & \vdots & \vdots & \ddots & 0 \\ 0 & 0 & 0 & 0 & 0 & 0 & \cdots & 1 \end{pmatrix} & & \end{matrix},$$

and

$$C_0 = \begin{matrix} & & \bar{\sigma}(n-1) - n & & \bar{\sigma}(n) - n & & n-1 & n \\ \bar{\sigma}(n-1) - n & \begin{pmatrix} \cdots & \cdots & 0 & \cdots & 0 & \cdots & 0 & 0 \\ 0 & 0 & \lambda_{\bar{\sigma}(n-1)-n}^1 & \cdots & \lambda_{\bar{\sigma}(n)-n}^1 & \cdots & \lambda_{n-1}^1 & \lambda_n^1 \\ \vdots & \vdots & \vdots & \ddots & \vdots & \ddots & \vdots & \vdots \\ 0 & 0 & \lambda_{\bar{\sigma}(n-1)-n}^2 & \cdots & \lambda_{\bar{\sigma}(n)-n}^2 & \cdots & \lambda_{n-1}^2 & \lambda_n^2 \\ \vdots & \vdots & 0 & \ddots & 0 & \ddots & 0 & 0 \end{pmatrix} & \end{matrix},$$

The elements $C_0[i_w, i_w] = 1$, where $C_0[i_w, i_w]$ are the element in i_w row and i_w columns of C_0 . Other elements in C_0 are zero. It is obvious that the permutation on the box will not affect C_0 and all the delta functions associate with C_0 . Furthermore all the parameters α_I are fixed by the delta functions in the box. And none of vertices and internal lines outside the box in the on-shell diagram can be affected by permutations of the external legs. Hence all BCFW bridges are invariant under the external leg permutations, which in turn implies that the Grassmannian cell C is invariant under the permutations. We can make a stronger generalization: any permutations of two legs attached to a box in bipartite diagram will not affect the Grassmannian cell. The proof is completely analogous; an example will be presented in Section 5.

2.3 Permutation relations for NMHV amplitudes—a twin-box connected by a BCFW bridge

In general, however, not any two consecutive legs can enjoy direct connection to a box. From NMHV amplitude to more general amplitudes, the next basic object arisen in a permutation of two adjacent legs is a twin-box with the two permuting legs connected by a BCFW bridge in Fig 5, showing the first NMHV example of a six point Yangian invariant corresponding to the permutation $\sigma_1 = \{4, 5, 6, 8, 7, 9\}$ with 5 and 6 being the permuting legs. According to

$$\begin{aligned} Y_{\sigma_1}^{(3)}(o2) &\equiv \frac{A^{MHV}(o2)\bar{Y}_{\sigma_1}^{(3)}(o2)}{A^{MHV}(o2)} \\ &= \frac{\langle 2365 \rangle^{o2} \langle 3651 \rangle^{o2} \langle 6512 \rangle^{o2} \langle 1236 \rangle^{o2} \langle 5123 \rangle^{o2}}{\delta(\langle 2365 \rangle^{o2} \tilde{\eta}_1 + \langle 3651 \rangle^{o2} \tilde{\eta}_2 + \langle 6512 \rangle^{o2} \tilde{\eta}_3 + \langle 5123 \rangle^{o2} \tilde{\eta}_6 + \langle 1236 \rangle^{o2} \tilde{\eta}_5)} \quad (2.15) \end{aligned}$$

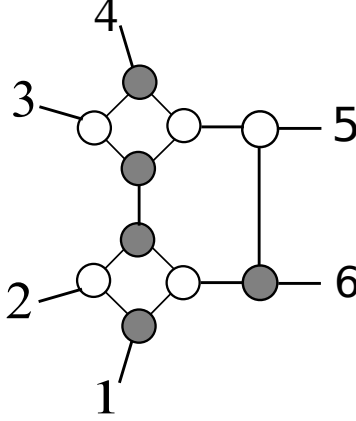


Figure 5. In a typical NMHV diagram, a pair of external legs, marked "5" and "6," can be made to connect to a basic twin-box with a BCFW bridge by judicious applications of the permutation relations of Yangian Invariants

and a similar equation for $Y_{\sigma_1}^{(3)}(o1)$ ³, the permutation relation is easy to obtain,

$$\begin{aligned} \bar{Y}_{\sigma_1}^{(3)}(o2) &= \frac{\langle 2356 \rangle^{o1} \langle 3561 \rangle^{o1} \langle 5612 \rangle^{o1} \langle 6123 \rangle^{o1} \langle 1235 \rangle^{o1}}{\langle 2365 \rangle^{o2} \langle 3651 \rangle^{o2} \langle 6512 \rangle^{o2} \langle 5123 \rangle^{o2} \langle 1236 \rangle^{o2}} \\ &\times \frac{1}{(\langle 1235 \rangle^{o2})^4} \int d^4 \bar{\eta}_6 \delta(\langle 1235 \rangle^{o2} \bar{\eta}_6 - \sum_{i=1}^6 c_i \tilde{\eta}_i) \bar{Y}_{\sigma_1}^{(3)}(o1), \end{aligned} \quad (2.16)$$

where $o2 = (1, 2, 3, 4, 6, 5)$, $o1 = (1, 2, 3, 4, 5, 6)$ and $c_1 = \langle 2365 \rangle^{o2} - \langle 2356 \rangle^{o1}$, $c_2 = \langle 3651 \rangle^{o2} - \langle 3561 \rangle^{o1}$, $c_3 = \langle 6512 \rangle^{o2} - \langle 5612 \rangle^{o1}$, $c_4 = 0$, $c_5 = \langle 1236 \rangle^{o2} - \langle 6123 \rangle^{o1}$, $c_6 = \langle 5123 \rangle^{o2}$.

In fact for a Yangian Invariant in NMHV amplitudes, a bipartite diagram is composed of BCFW-bridged box glued with k -preserving inverse soft factor $Y_n^{(3)} = Y_6^{(3)} \underbrace{\odot Y_3^{(1)} \odot \dots \odot Y_3^{(1)}}_{n-6}$. This is because we can choose a BCFW bridge for at least one pair of consecutive legs such that $Y_{n_L}^{k_L}$ and $Y_{n_R}^{k_R}$ with $n_L > 3$, $n_R > 3$ and $k_L = k_R = 2$. And according to the analysis in Section 2.1 the general structure and the permutation relation of an on-shell diagram in NMHV is as shown in Fig. 6.

For general amplitudes beyond NMHV this permutation relation for the BCFW-bridged twin-box can easily be shown to exist for a class of Yangian invariants. We

³This is the form of Yangian invariants in momentum twistor space, and we will mainly discuss amplitudes in momentum twistor space in his paper. Brief introduction of momentum twistor space is in Appendix A

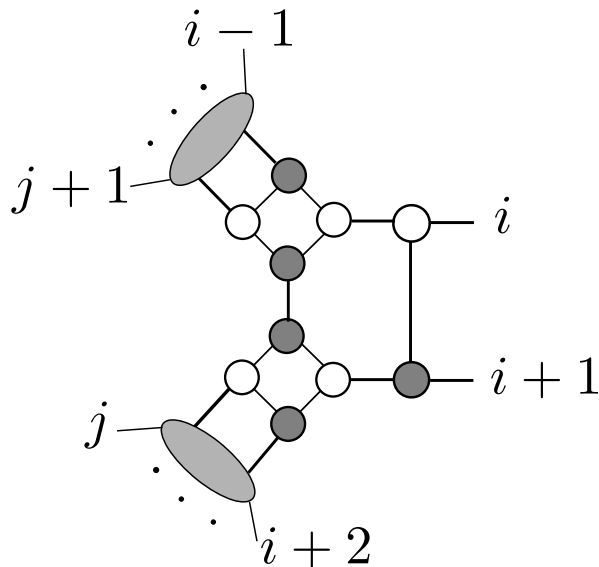


Figure 6. Bridged bi-box with permutation legs $i, i + 1$.

shall establish a convenient criterion for them. To this end, we define a revised BCFW-Bridge decomposition [35].

BCFW-Bridge decomposition of a bridged twin-box: Staring with a given permutation σ , we mark two consecutive legs i and $i+1$ and other two legs $\sigma(i) \bmod n, \sigma(i+1) \bmod n$. Now one chooses another $n - 6$ legs, other than the four chosen ones. The left 6 legs are left fixed if $\sigma(i) \bmod n \neq i$ and $\sigma(i+1) \bmod n \neq i+1$ and the the box contact condition (2.8) does not hold. If σ for other legs is not a “dressed” identity ⁴ we decompose σ as $(j_1 j_2) \circ \sigma'$, where $1 \leq j_1 < j_2 \leq n$, $\sigma(j_1) < \sigma(j_2)$, $j_1 \neq i, i+1$, $j_2 \neq i, i+1$ and j_1, j_2 are separated only by marked legs or legs $i, i+1$, keeping the order of the 6 fixed legs. This procedure is repeated until σ becomes the identity for all the mobile legs and the resultant permutation is denoted by $\bar{\sigma}$.

If $\bar{\sigma}$ is a permutation of Y_6^3 then the bipartite diagram is of the form shown in Fig. 7. When we permute the legs “ i ” and “ $i+1$ ”, the effect of the permutation on the Grassmannian matrix C will be partially blocked by the box. In fact the total number of BCFW bridges acting on a bridged twin-box is $2n - 12$; and we obtain

$$C = C_0 \mathcal{B}(i_8, j_8; \alpha_8) \cdot \mathcal{B}(i_9, j_9; \alpha_9) \dots \mathcal{B}(i_I, j_I; \alpha_I) \dots \mathcal{B}(i_{2n-4}, j_{2n-4}; \alpha_{2n-4}). \quad (2.17)$$

Similar to a permutation on the box all the parameters α_I are fixed by delta

⁴For example, for $n = 6, k = 3$, a “dressed” identity is $\{7, 8, 3, 10, 5, 6\}$.

functions of momentum conservation in the bridged twin-box. None of the vertices and internal lines outside of the bridged twin-box are affected by the permutations of the external legs. Hence all BCFW bridges are invariant under these permutations. Nevertheless one row in C_0 does change while the other rows of are invariant under a leg permutation on the twin-box. Such transformation relations on C is therefore useful for classifying Yangian invariants related by a given permutation of legs.

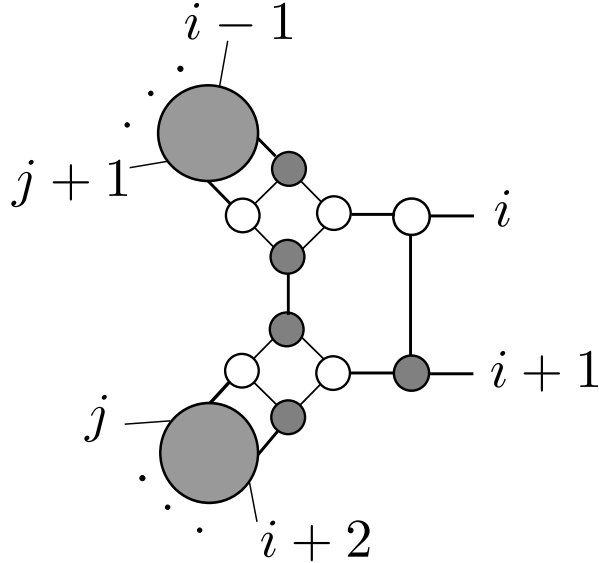


Figure 7. Bridged bi-box with permutation legs $i, i+1$.

3 Unitarity cuts and generalized unitarity cuts

In $\mathcal{N} = 4$ supersymmetry Yang-Mills theory “single cut” is an efficient way of constructing all loop integrands for planar loop amplitudes. However in the nonplanar case the resultant diagram after a single cut is often not a well-defined Feynman diagram. One can also view this problem as a difficulty to endow the loop momentum with a canonical definition because the nonplanar leg(s) can fall between any two planar legs inside a loop. In fact all such possibilities should be taken into account.

The general loop amplitudes after the unitarity cuts and generalized unitarity cuts can be regarded as tree level amplitudes being glued together. Hence the unitarity and generalized unitarity cut loop amplitudes are well-defined and can be taken as the foundation to construct the integral of the amplitudes. From this point of view, the major difference for planar and nonplanar diagrams under unitarity cuts is that all

the gluing lines in each tree-level amplitude are adjacent for planar diagrams while in nonplanar diagrams at least a pair of gluing lines is nonadjacent. Furthermore, for the unitarity cuts, together with the on-shell diagrams for the tree-level amplitudes, it is also possible to construct the integrand of the general loop amplitudes systemically, which we will discuss in Section 4.

3.1 Unitarity cut

Given a nonplanar diagram one should consider all possible diagrams resulted from the nonplanar leg(s) taking all probable positions when traversing around the loop. The simplest example is the four-point one-loop with one nonplanar leg—which we shall call the “(3+1)” case for short in the rest of the article—as shown in Fig. 8. The nonplanar

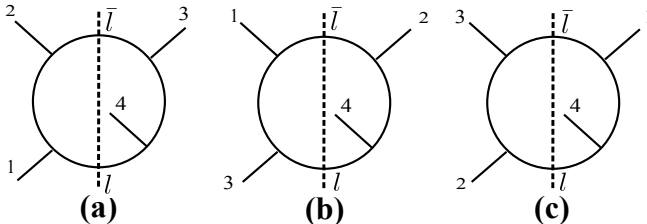


Figure 8. Three possible positions of the nonplanar leg and a possible unitarity cut in each case.

leg can take up three different positions; and there are two possible unitarity cuts.

The ambiguity in defining the loop momentum is resolved as follows: if we start with the external line marked “4” we can call the momentum on the first cut loop line l , and \bar{l} the loop momentum on the other cut line. In the clockwise order for the color-ordered amplitudes one easily checks that in each resultant tree diagram the momentum is well defined for each of the external legs.

We can keep track of the order of unitarity cuts as well: under each cut the diagram will be divided into a diagram with one fewer loops in addition to a tree-level diagram. A typical higher loop case is shown in Fig. 9.

The ambiguity in the definitions of the loop momenta is resolved by a series of unitarity cuts. In fact we can define each loop momentum clockwise from a reference external line. For the typical example in (a) of Fig. 9, if we start with the external line marked “1”—in the clockwise order for the color-ordered amplitudes—we can call the momentum on the first cut loop-line l_1 and \bar{l}_1 the loop momentum on the other cut line. After setting l_1 as the reference line in the first loop the momentum on the

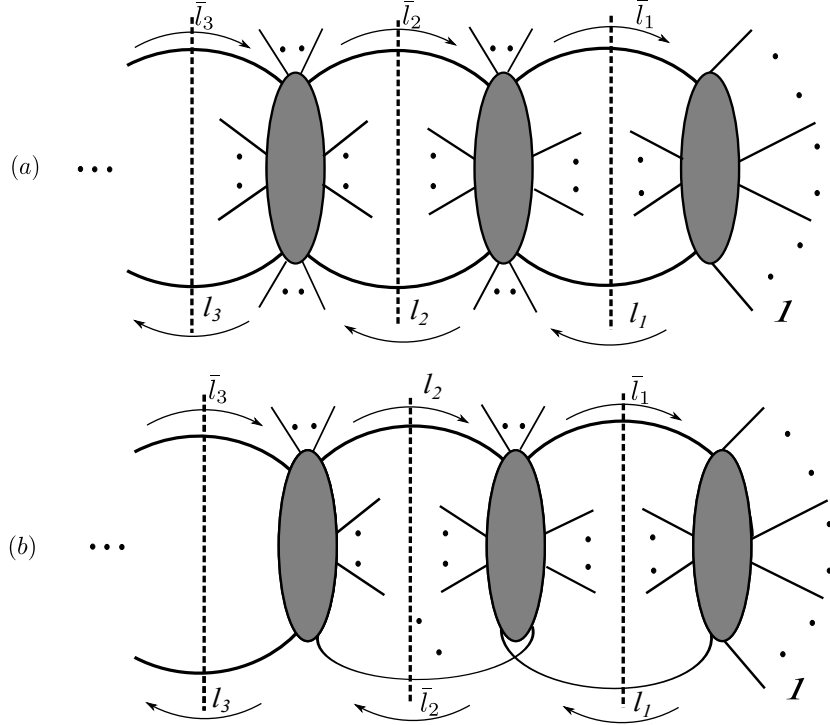


Figure 9. Unitarity cuts for a higher loop nonplanar diagram.

other cut line becomes $\bar{l}_1 = l_1 - P_R$ where P_R being the sum of all external momenta between these two cut lines. The momenta on the second loop can thus be fixed to be l_2 and $\bar{l}_2 = l_2 - P'_R$ with P'_R denoting the sum of all the external momenta to the right of l_2 , and so forth.

Obvious in this construction, topological information of nonplanarity is preserved: one unitarity cut can only fix two components of the 4-momentum integrals leaving the other two integrations unconstrained. Furthermore, the integrand under the unitarity cut is also well-defined. This means that the integrand contains enough information for the characterization of the loop topology of nonplanar diagrams. And the loop topology and geometric properties of the underlying Grassmannian arisen in nonplanar amplitudes will be manifest once we construct nonplanar amplitudes in on-shell bipartite diagrams [35].

The permutation relations of bipartite on-shell diagrams—each of them corresponding to a Yangian with its gauge invariance—are instrumental in constructing the whole amplitude from unitarity cut or generalized unitarity cut diagrams. To construct the bipartite on-shell diagrams after a unitarity cut we need to convert each resultant tree

amplitudes in Fig. 9 into the corresponding bipartite diagrams. The loop lines connecting the tree amplitudes now denote the same integration as the internal lines in tree-level bipartite on-shell diagrams. Since the construction of bipartite on-shell diagram for each tree level diagram is well established in [35], we only need to verify the gluing lines in bipartite diagram are equivalent to a unitarity cut of loop amplitudes.

In the language of bipartite on-shell diagram, the gluing line represents an extra integral:

$$\int \frac{d^2\lambda_{l_1} d^2\tilde{\lambda}_{l_1}}{\text{vol}(GL(1))} d^4\tilde{\eta}_{l_1} \int \frac{d^2\lambda_{l_2} d^2\tilde{\lambda}_{l_2}}{\text{vol}(GL(1))} d^4\tilde{\eta}_{l_2} A_L^S A_R^S \quad (3.1)$$

where $A_L^S = A_L \delta^{2 \times 2}(l_1 + P_L - l_2) \delta^{2 \times 4}(\lambda_L \cdot \tilde{\eta}_L)$, $A_R^S = A_R \delta^{2 \times 2}(-l_1 + P_R + l_2) \delta^{2 \times 4}(\lambda_R \cdot \tilde{\eta}_R)$. This can be further simplified,

$$\int \langle \lambda d\lambda \rangle [\tilde{\lambda} d\tilde{\lambda}] d^4\tilde{\eta}_{l_1} \frac{P_L^2}{\langle \lambda | P_L | \tilde{\lambda} \rangle^2} d^4\tilde{\eta}_{l_2} A_L A_R \delta^{2 \times 2}(P_R + P_L) \delta^{2 \times 4}(\lambda_L \cdot \tilde{\eta}_L) \delta^{2 \times 4}(\lambda_R \cdot \tilde{\eta}_R) \quad (3.2)$$

which is exactly the expression of a loop level amplitude after a unitarity cut.

Let us turn, again, to our lovely “3+1” example (Fig. 8), the bipartite on-shell diagrams correspond to the tree amplitudes resulted from a unitarity cut are shown in Fig. 10. After the cuts, only two four-point tree amplitudes are left. Each tree

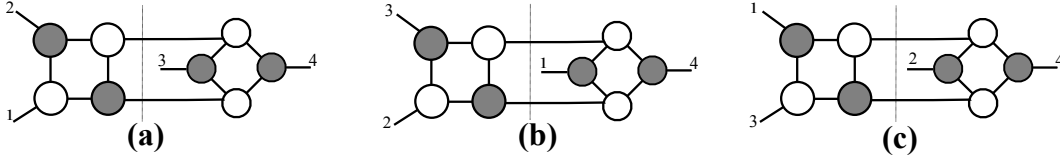


Figure 10. The bipartite on-shell diagrams of an s-channel cut (a), and a t-channel cut (b), and a u-channel cut (c). **Note:** In our convention a horizontal square denotes the planar tree amplitude while a rhombus (at 45 degrees) denotes a nonplanar amplitude with the plane of rhombus being perpendicular to the plane of the paper where the points marked “3” and “4” are at equal distance from the vertical edges of the (planar) square.

amplitude is a box. Now we can add two lines to connect these two boxes to represent the cut amplitude. There are three different cuts—the s-channel cut, the t-channel cut, and the u-channel cut. Each of them can be represented in on-shell diagrams in the ways shown in Fig. 10.

We now present our strategy for constructing the full scattering amplitudes in the bipartite on-shell language for the corresponding the nonplanar Feynman diagrams. In this work we only focus on the one-loop diagrams. We would like to stress that our strategy can be extended to the higher loops cases, with generalized unitarity cuts,

in a straightforward way. Detailed descriptions, together with carefully worked out examples, of the one-loop amplitudes will be presented in Section 4.

- Perform all possible unitarity cuts on a given nonplanar Feynman diagram.
We convert the resultant diagrams from each possible (series of) unitarity cuts into on-shell bipartite diagrams. Each bipartite diagram corresponds to a Yangian invariant.
- Remove all unphysical poles in loops, the structures of which depend on the loop momenta.
They occur because Yangian invariants in general contain unphysical poles. However the unphysical poles will cancel each other upon summing over all Yangian invariants of a given amplitude—only physical poles remain. Furthermore the unphysical poles in loops are not allowed in the total amplitudes. We need to ensure that no unphysical poles of the loop momenta appear in the final expressions.
- Sum over all the inequivalent terms from each series of unitarity cuts.
After removing the unitarity cut conditions, we will get an integral with respect to all the loop momenta. If there appears the same integral when reconstructing from a different unitarity cut then it suffices to count it once.

3.2 Generalized unitarity cuts

Generalized unitarity cut can also be used to construct the full loop level amplitudes. For $\mathcal{N} = 4$ SYM after a quadruple cuts on each loop only the leading singularity of the loop level amplitudes remains. All loop momenta are fixed by the cut constraints. Absent is the possibility of having a rational function in loop momenta. However, from the bipartite on-shell diagrams, lots of geometric information of the Grassmannian can be read off from the leading singularity, as shown in Fig. 11.

In a one loop nonplanar diagram, Fig. 12, the leading singularity is of form

$$\int \prod_{i=1}^4 \frac{d^2 \lambda_i d^2 \tilde{\lambda}_i}{\text{vol}(GL(1))} d^4 \tilde{\eta}_i \mathcal{A}_1^S(1 \cdots 2 \cdots) \mathcal{A}_2^S(2 \cdots 3 \cdots) \mathcal{A}_3^S(3 \cdots 4 \cdots) \mathcal{A}_4^S(4 \cdots 1 \cdots). \quad (3.3)$$

Similar to the case of planar diagrams the leading singularities of nonplanar diagrams can also be identified as residues of the Grassmannian integral, a specific example of which will be given in Section 5.

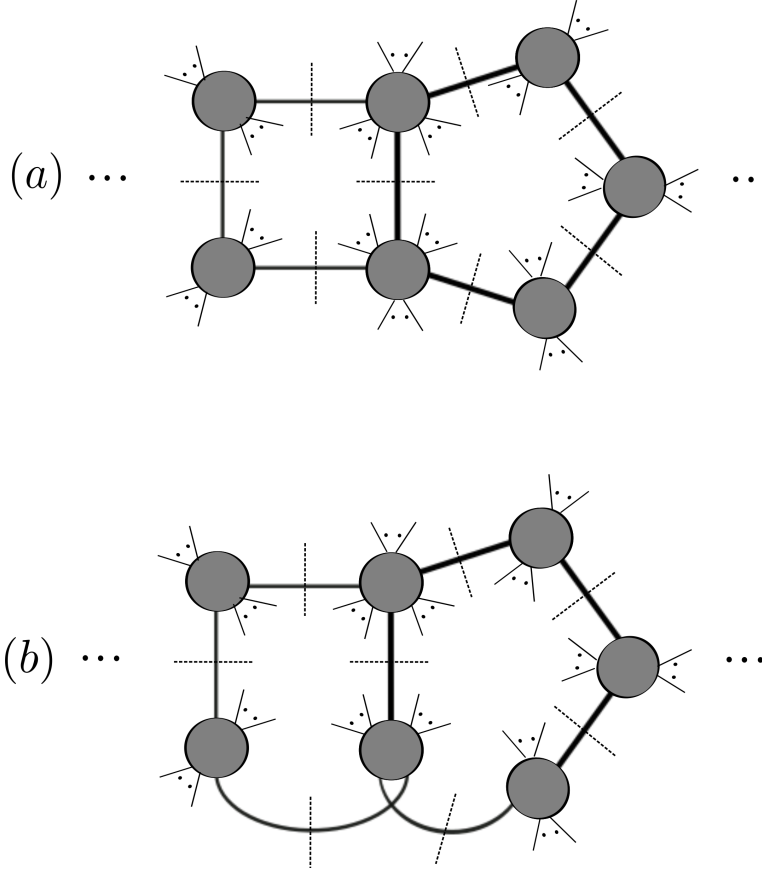


Figure 11. Leading singularity in general loop amplitudes under generalized unitarity cuts.

In the case of $\mathcal{N} = 4$ SYM double unitarity cuts (quadruple cuts) can fully determine the full amplitudes. Compared to a unitarity cut double unitarity cuts are more convenient to the full amplitudes' reconstruction because all the poles in loop momenta are automatically physical upon such cuts. Furthermore different double unitarity cuts lead to different scalar integrals: we do not need to consider equivalent integrals as we do with unitarity cuts. The general procedures of reconstructing the full amplitudes by double cuts are as follows.

- Perform all possible double unitarity cuts on the nonplanar Feynman diagrams with loops. For each possible series of quadruple cuts we convert the resultant tree-level amplitudes to the bipartite diagrams. We then glue the cut loop lines according to the Feynman diagram. Similar to the planar case these reproduce the leading singularities of the nonplanar amplitudes.
- Transform the nonplanar leading singularities into planar ones by the permutation

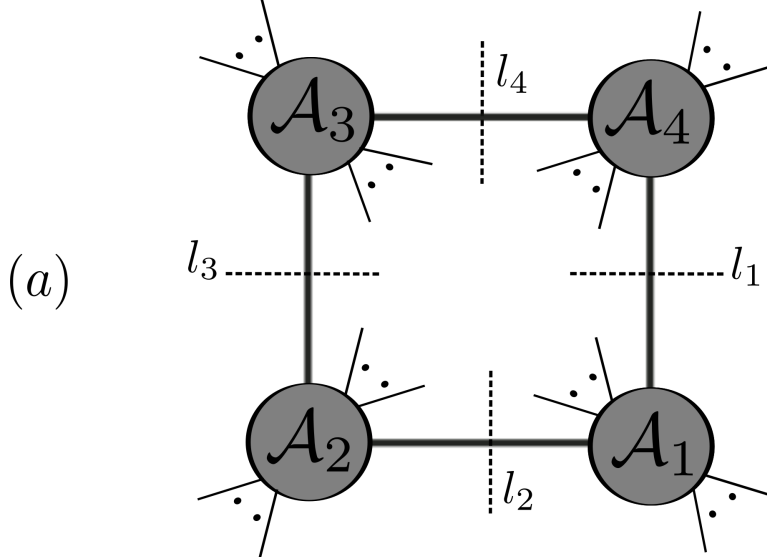


Figure 12. Leading singularity in one loop amplitudes under generalized unitarity cuts.

relations of the Yangian invariants.

- Multiply the leading singularities by a standard integral.
- Sum over all contributions from each series of quadruple cuts.
- To elucidate the geometric properties of the Grassmannian we group terms according to their underlying Grassmannian geometry.

4 MHV Loop Amplitudes

In $U(N)$ Yang-Mills theory, the one loop amplitudes can be decomposed as [52]

$$\begin{aligned}
 A_n^{1\text{-loop}}(\{a_i\}) &= \sum_{\sigma \in S_n/Z_n} N_c \text{Tr}(T^{a_{\sigma(1)}} \dots T^{a_{\sigma(n)}}) \mathcal{A}_{n;1}(\sigma(1), \dots, \sigma(n)) \\
 &+ \sum_{c=2}^{\lfloor n/2 \rfloor + 1} \sum_{\sigma \in S_n/S_{n;c}} \text{Tr}(T^{a_{\sigma(1)}} \dots T^{a_{\sigma(c-1)}}) \text{Tr}(T^{a_{\sigma(c)}} \dots T^{a_{\sigma(n)}}) \mathcal{A}_{n;c}(\sigma(1), \dots, \sigma(n)),
 \end{aligned} \tag{4.1}$$

where $\mathcal{A}_{n;c}$ are the partial amplitudes, Z_n and $S_{n;c}$ are the subsets of S_n that leave the corresponding single and double trace structures invariant, and $\lfloor x \rfloor$ is the greatest integer less than or equal to x . In this paper the diagrams corresponding to single trace and double trace partial amplitudes are regarded as planar and non-planar diagrams

respectively. We will focus on the partial amplitudes of planar diagram, $\mathcal{A}_P \equiv \mathcal{A}_{n,1}$, as well as nonplanar diagrams, $\mathcal{A}_{NP} \equiv \mathcal{A}_{n,2}$, of 4-point, 5-point interactions.

4.1 MHV planar amplitudes and unitarity cuts

Using single cuts techniques, Arkani-Hamed et al has thoroughly studied planar amplitudes of all loops in momentum twistor space [21]. On the other hand Bern et al introduced unitarity cuts as a way to reconstruct planar MHV amplitudes in momentum space [5]. At this point, however, no systematic method of MHV amplitudes reconstruction from unitarity cuts in momentum twistor space exists.

In this section, we present a detailed method of constructing MHV one-loop amplitudes from unitarity cuts. We build relations of bipartite on-shell diagrams and express them in momentum twistor space. This method leads us naturally to simple results without unphysical poles, in addition to the final integrands being the same as those from single cuts. This is to be contrasted with the way proposed by Bern et al [5] in dealing with the box integrals. Given these advantages it is thus a meaningful exercise to study MHV amplitudes in momentum twistor space together with unitarity cuts. The steps of reconstruction of MHV one-loop amplitudes from unitarity cuts are:

- I Draw the on-shell diagrams of each amplitude under unitarity cuts.
- II Add BCFW bridges to remove the unitarity cut constraints and directly write down the integrand form in momentum twistor space.
- III Convert un-physical poles in the previous form to physical ones.
- IV Combine results from different cuts to get the final integrands.

Example: Integrands of five-point one loop amplitudes

Now we give an example to explicit the above procedure. First non-trivial example is five-point planar amplitude.

Step I: In five-point situation, there are five different unitarity cuts $A_c(i, i+1|i+2, i+3, i+4)$, $i = 1, 2, 3, 4, 5$. $A_c(12|345)$, for instance, can be constructed as gluing two tree level amplitudes $A_L(12|\bar{l})$ and $A_R(\bar{l}|345)$ as shown in Fig. 9 for the general case. The corresponding on-shell diagrams is shown in (a) of Fig. 13.

Step II: Add BCFW bridges to $(2 \hat{3})$ and $(1 \hat{5})$ to remove the cut constraints (shown in Fig. 13). We can simply write the integrand in momentum twistor space,

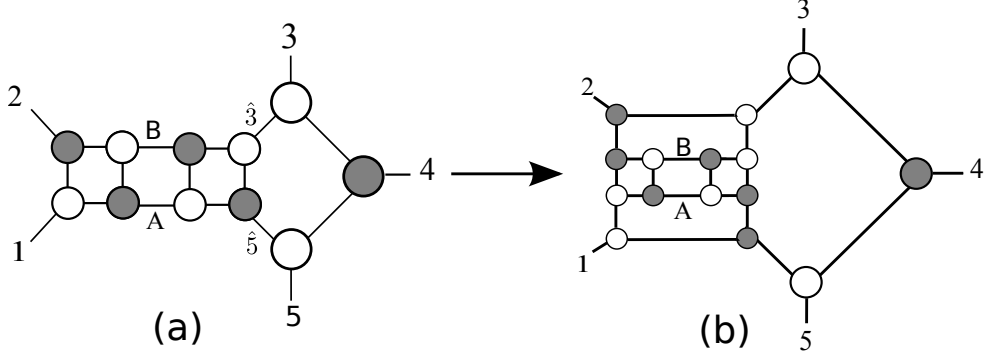


Figure 13. (a) shows the on-shell diagram of $A_c(12|345)$, and (a) transforming to (b) indicates a new way of adding BCFW bridges to remove the cut constraints (the step II). A and B denote two cut lines.

based on the four-point one-loop situation, as

$$\mathcal{A}_0(1, 2|3, 4, 5) = \frac{-\langle 1235 \rangle^2}{\langle AB12 \rangle \langle AB23 \rangle \langle AB35 \rangle \langle AB51 \rangle}, \quad (4.2)$$

where A and B denote the points of the cut lines in momentum twistor space (Appendix A).

Step III: There are unphysical poles in the denominator of the previous equation, such as $\langle AB35 \rangle$. These poles can be converted to physical ones using unitarity condition, $\langle AB23 \rangle = 0$, $\langle AB51 \rangle = 0$. We could build a relation between $\frac{1}{\langle AB35 \rangle}$ and $\frac{1}{\langle AB34 \rangle \langle AB45 \rangle}$ as

$$\mathcal{A}_1(1, 2|3, 4, 5) = \frac{\langle AB24 \rangle \langle 3512 \rangle \langle 1345 \rangle + \langle AB34 \rangle \langle 5123 \rangle \langle 1245 \rangle}{\langle AB12 \rangle \langle AB23 \rangle \langle AB34 \rangle \langle AB45 \rangle \langle AB51 \rangle} \quad (4.3)$$

Step IV: Repeat the above three steps on another unitarity cut, we obtain the result of another cut $\mathcal{A}_1(2, 3|4, 5, 1)$ as

$$\mathcal{A}_1(2, 3|4, 5, 1) = \frac{\langle AB25 \rangle \langle 3451 \rangle \langle 4123 \rangle + \langle AB51 \rangle \langle 3452 \rangle \langle 4123 \rangle}{\langle AB12 \rangle \langle AB23 \rangle \langle AB34 \rangle \langle AB45 \rangle \langle AB51 \rangle}. \quad (4.4)$$

Now we need to combine these two results from different cuts. Z_5 could be expanded based on Z_1, Z_2, Z_3, Z_4 , to get $\langle AB25 \rangle \langle 4123 \rangle = \langle AB23 \rangle \langle 4125 \rangle + \langle AB24 \rangle \langle 5123 \rangle$ where $\langle AB12 \rangle$ vanishes due to unitarity cut condition. Obviously the term $\langle AB24 \rangle$ is the same in these two terms, so we only need to count its contribution once. Other terms in these two equations could be directly added together not affecting the results under

both unitarity cuts. Combining other three cuts with the same method we get the final integrand of planar one loop five-point MHV amplitude as

$$\mathcal{A}_P(1, 2, 3, 4, 5) = \frac{-\langle AB24 \rangle \langle 2351 \rangle \langle 4351 \rangle}{\langle AB12 \rangle \langle AB23 \rangle \langle AB34 \rangle \langle AB45 \rangle \langle AB51 \rangle} \quad (4.5)$$

$$- \frac{\langle AB23 \rangle \langle 2451 \rangle \langle 3451 \rangle + \langle AB34 \rangle \langle 2451 \rangle \langle 2351 \rangle + \langle AB51 \rangle \langle 2345 \rangle \langle 2341 \rangle}{\langle AB12 \rangle \langle AB23 \rangle \langle AB34 \rangle \langle AB45 \rangle \langle AB51 \rangle},$$

which is the same result as obtained from single cuts in [21].

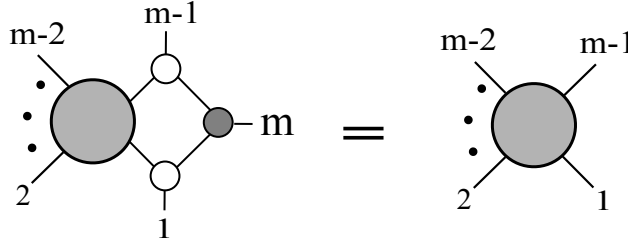
This simple example serves to illustrate our strategy to compute Yang-Mills integrands using unitarity cuts. This is to be contrasted with the single cuts method proposed by Arkani-Hamed et al [21, 22] as well as constructing the scattering amplitudes integral after unitarity-cutting the Feynman diagrams as done by Bern et al at a much earlier attempt [5, 6]. We shall proceed with a general discussion of the higher-point results in the rest of the section.

Property of MHV planar amplitudes under unitarity cuts

To study MHV loop amplitudes under unitarity cuts we first tackle MHV tree amplitudes, of which Yangian Invariant is $Y_n^{(2)} = Y_4^{(2)} \underbrace{\odot Y_3^{(1)} \odot \dots \odot Y_3^{(1)}}_{n-4}$. The relationship between n-point Yangian Invariant (not necessarily MHV) and (n-1)-point Yangian Invariant after stripping off one $\odot Y_3^{(1)}$ is simply⁵

$$Y_{m-1}^{(k)}(Z_1, \dots, Z_{m-1}) = Y_m^{(k)}(Z_1, \dots, Z_{m-1}, Z_m) \quad (4.6)$$

in momentum twistor space, which can, in turn, be represented in on-shell bipartite diagrams as



The planar part, in general, can be reduced to a very simple form (which we call a basic “twin-box”) shown in Fig. 14.

⁵We have omitted the MHV tree amplitude factor from the full amplitude in momentum space.

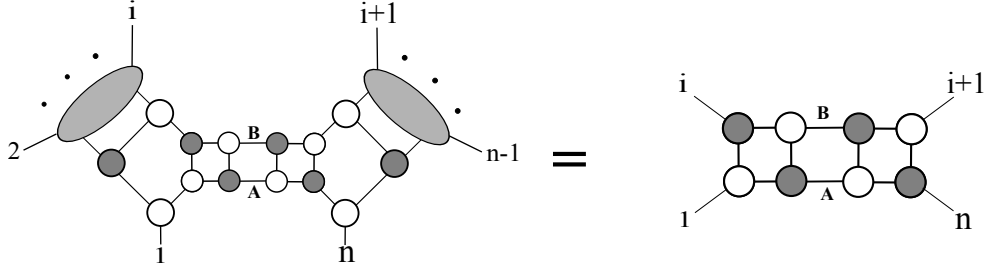


Figure 14. An n -point MHV one-loop planar amplitude after unitarity cuts can be converted to a basic “twin-box” with only four external legs.

We can therefore obtain the MHV amplitude after unitarity cuts as

$$A_c(1, 2, \dots, i|i+1, \dots, n) = A_c(1, i|i+1, n), \quad (4.7)$$

where A_c denotes the amplitude under each of the possible unitarity cuts. ‘|’ denotes the cut line between these two legs and the other cut line between the first and last legs in the bracket. This relation shows that an n -point MHV amplitude is the same as a four-point amplitude under unitarity cuts in momentum twistor space.

Removing the unitarity cut constraints

The standard way of reconstructing amplitudes from single cuts is by adding BCFW bridges across cut lines on a pair of external legs. For amplitudes under unitarity cuts we do not necessarily have to add bridges on external legs. In fact the unitarity-cut amplitudes in MHV case can be reduced to the basic “twin-box” in momentum twistor space (Fig. 14). They contain all the essential information of the whole amplitudes after unitarity cuts. This is also apparent in momentum space. After four internal integrals, all δ -functions from the three blocks vanish, reducing the number of external legs by one. Recursively, the whole amplitude can be reduced to a basic “twin-box” with four new external on-shell momenta. This means that adding bridges to the “twin-box” recover the same result from a unitarity cut. This new way of adding BCFW bridges will greatly simplify our subsequent computations. In on-shell diagram it amounts to Fig. 15.

The final result of this planar part is, thus, nothing but a one-loop four-point planar amplitude. We denote the cut loop momenta, l and \bar{l} , by the variables A and B in

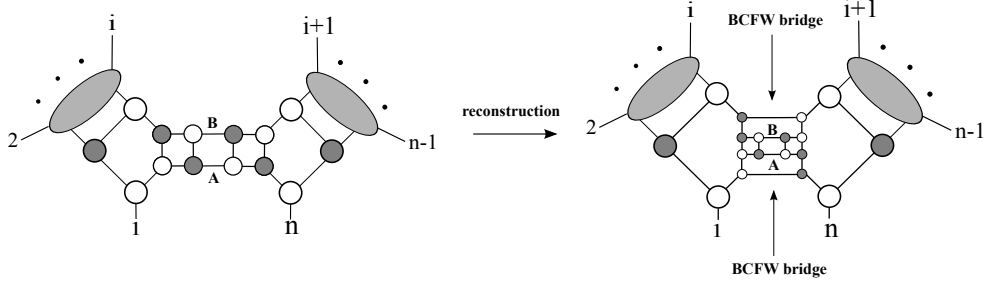


Figure 15. A new way of adding BCFW bridges with simpler expressions of integrands.

momentum twistor space.⁶

$$\mathcal{A}_0(1, \dots, i|i+1, \dots, n) = \frac{\langle 1ii+1n \rangle \langle ii+1n1 \rangle}{\langle AB1i \rangle \langle ABii+1 \rangle \langle ABi+1n \rangle \langle ABn1 \rangle}, \quad (4.8)$$

where \mathcal{A}_0 denotes the amplitude after adding two BCFW bridge to the “twin-box”.

Conversion from unphysical poles to physical ones:

Since the form of planar amplitudes after reconstruction is actually from a four-point (Z_i, Z_{i+1}, Z_1, Z_n) (with the subscripts denoting the momenta of the four legs connected to the “twin-box” as in Fig. 14) amplitude, some propagators, say $\langle ABi+1n \rangle$ and $\langle ABin \rangle$, becomes unphysical poles inside an n -point amplitude (A and B as before denote the loop momenta, l and \bar{l} , in the momentum twistor space.).

We at present present a way to convert unphysical poles to physical ones using the unitarity cut condition. We show by an example of an amplitude with color ordering $(1, 2, \dots, n)$ and unitarity cut $\langle ABii+1 \rangle \langle ABjj+1 \rangle$ as shown in Fig. 16. In a particular order, this is just a planar diagram, we can discuss the integrand. The unitarity cut condition is $\langle ABii+1 \rangle = 0, \langle ABjj+1 \rangle = 0$. And the poles $\langle ABi+1j \rangle$ and $\langle ABj+1i \rangle$ become unphysical.

Imposing the unitarity cut condition,

$$\frac{\langle ii+1jj+1 \rangle}{\langle ABi+1j \rangle} = \frac{\langle ABi+1i+2 \rangle \langle ij-1jj+1 \rangle + \langle ABii+2 \rangle \langle j-1jj+1i+1 \rangle}{\langle ABi+1i+2 \rangle \langle ABj-1j \rangle}, \quad (4.9)$$

where all of the poles in the denominator are physical. Here we convert it to another form related to the intersection of two planes $(ii+1i+2)$ and $(j-1jj+1)$, which is useful

⁶We omit the terms related to integral variables $\int \langle ABd^2z_A \rangle \langle ABd^2z_B \rangle$ in this paper. Since we deal with the integrand of amplitudes, we leave this as a common factor of in the integrand.

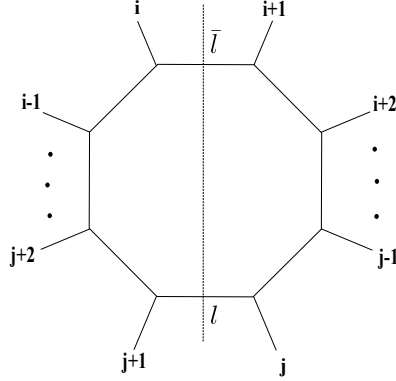


Figure 16. A unitarity cut n -point planar amplitude with color ordering $(1, 2, \dots, n)$

in the latter discussion.

$$\frac{\langle ii + 1jj + 1 \rangle}{\langle ABi + 1j \rangle} = \frac{\langle AB(ii + 1i + 2) \cap (j - 1jj + 1) \rangle}{\langle ABi + 1i + 2 \rangle \langle ABj - 1j \rangle}. \quad (4.10)$$

We use the same method to deal with pole $\langle ABj + 1i \rangle$. According to (4.10) and combining these two parts,

$$\begin{aligned} \mathcal{A}_{c_{j+1i}} &\equiv \mathcal{A}_{c_{j+1i}}(j + 1, \dots, i | i + 1, \dots, j) \\ &= \frac{-\langle AB(i - 1ii + 1) \cap (j - 1jj + 1) \rangle \langle AB(jj + 1j + 2) \cap (i - 1ii + 1) \rangle}{\langle ABi - 1i \rangle \langle ABii + 1 \rangle \langle ABi + 1i + 2 \rangle \langle ABj - 1j \rangle \langle ABjj + 1 \rangle \langle ABj + 1j + 2 \rangle}. \end{aligned} \quad (4.11)$$

In this paper c_{ij} with $1 \leq i < j \leq n - 1$ denotes the cuts that divide the external lines into two groups $i \cdots j$ and $j + 1 \cdots i - 1$. For convenience, we also use C_{ij} to denote a cut set containing all the cuts $c_{12} \cdots c_{ij}$ in the union order. The corresponding $\mathcal{A}_{C_{ij}}$ denote the union of all the integrands from the cuts in C_{ij} . And $\mathcal{A}_{c_{ij}}$, $\mathcal{A}_{C_{ij}}$ may have the ambiguity of a rational function which will vanish under all the cuts in C_{ij} . We denote the corresponding arbitrary rational functions as $\mathcal{R}_{C_{ij}}$ or $\mathcal{R}_{c_{ij}}$.

Combination of different unitarity cuts

In the above paragraphs, we obtain an integrand \mathcal{A}_c from each cut amplitudes. Such integrand contains only physical poles and is well-defined up to rational functions which will vanish under unitarity cuts. In this paragraph, we need to find a way to get the rational function $\mathcal{A}_{C_{1n}}$ of the integrand such that it is equal to $\mathcal{A}_{c_{ij}}$ at the corresponding unitarity cuts. To this end, we define a operation \cup to the constructed integrand, which means an union of two integrand from different unitarity cuts. After the union of all the possible unitarity cuts, we get the integrand $\mathcal{A}_{C_{1n}}$ automatically.

According to the analysis in [5] on the unitary cut constructible for super-Yang-Mills theory, we can get $\mathcal{A}_P = \mathcal{A}_{C_{1n}}$.

Before the definition on \cup , we first define an union order for all the possible unitarity cuts as shown in Tab. 1, where the cut is label by one group of external legs in color order.

Table 1. Union order of unitarity cuts

c														
12	→	23		34	⋯	n-3	n-2		n-2	n-1				
		↓	↗	↓	⋯		↓		↓					
		123		234	⋯	n-4	n-3	n-2	n-3	n-2	n-1			
				↓	⋯		↓		↓					
				1234	⋯	n-5	n-4	n-3	n-2	↗	n-4	n-3	n-2	n-1
				⋮		⋮		⋮		⋮		⋮		⋮
						↓		↓		↓		↓		↓
						1⋯	n-2		2⋯	n-1				

Now we define the operation \cup on two rational functions in the function set group $\mathcal{A}_{c_{ij}}$ and $\mathcal{A}_{c_{i'j'}}$ as

$$\mathcal{A}_{C_{ij}} \cup \mathcal{A}_{C_{i'j'}}. \quad (4.12)$$

The operation can be divided into two steps: First, choose a proper $\mathcal{R}_{C_{ij}}$ such that all the terms $T_{(ij),(i'j')}$, which have one cut in C_{ij} and another cut in $C_{i'j'}$, are the same in both $\mathcal{A}_{C_{ij}}$ and $\mathcal{A}_{C_{i'j'}}$, while other terms $T_{(ij)}$ or $T_{(i'j')}$ in $\mathcal{A}_{C_{ij}}$ and $\mathcal{A}_{C_{i'j'}}$ can only have one cut either in C_{ij} or $C_{i'j'}$ respectively⁷; Second, add all the terms of same formula once and all other terms. Hence we can get

$$\mathcal{A}_{C_{ij}} \cup \mathcal{A}_{C_{i'j'}} = \sum T_{(ij),(i'j')} + \sum T_{(ij)} + \sum T_{(i'j')} + \mathcal{R}_{C_{ij} \cup C_{i'j'}}. \quad (4.13)$$

Such definition is similar for the union with $\mathcal{A}_{c_{ij}}$.

We unite the integrand from all the unitarity cuts in the union order one by one. We begin from the integrand $\mathcal{A}_{C_{12}}$ from the unitarity cut c_{12} , and then unite integrand

⁷In the following, we only verify this is possible for one-loop MHV amplitudes. And we will prove this for general ones in future work. Such procedure can also be generalized to other super Yang-Mills theory with lower super symmetry.

$\mathcal{A}_{C_{34}}$ and $\mathcal{A}_{C_{12}}$ and then others in the order. Finally we can obtain $\mathcal{A}_{C_{1n}}$. To this end, we first introduce some lemmas.

Lemma 1 For a pentagon integrand defined by five lines $\{L_{i-1i}, L_{ii+1}, L_{j-1j}, L_{jj+1}, L_{j+1j+2}\}$, where $L_{i-1i} = (Z_{i-1}Z_i)$ and a plane $\mathcal{P}_j = (Z_{j-1}Z_jZ_{j+1})$ (or $\mathcal{P}_i = (Z_{i-1}Z_iZ_{i+1})$) and an arbitrary plane $\mathcal{P}_x = (Z_{x_1}Z_{x_2}Z_{x_3})$

$$\frac{\langle AB\mathcal{P}_x \cap \mathcal{P}_j \rangle}{\langle ABi-1i \rangle \langle ABii+1 \rangle \langle ABj-1j \rangle \langle ABjj+1 \rangle \langle ABj+1j+2 \rangle},$$

and

$$\frac{\langle AB\mathcal{P}_i \cap \mathcal{P}_x \rangle}{\langle ABi-1i \rangle \langle ABii+1 \rangle \langle ABj-1j \rangle \langle ABjj+1 \rangle \langle ABj+1j+2 \rangle},$$

\exists lines $\{Y_2, Y_3, Y_4\}$ such that for any $Z_{m'}$ each integrand can be transformed to the following formulas

$$\begin{aligned} & \frac{\langle ABY_2 \rangle}{\langle ABi-1i \rangle \langle ABii+1 \rangle \langle ABj-1j \rangle \langle ABjj+1 \rangle \langle ABm'm'+1 \rangle} \\ & + \frac{\langle ABY_3 \rangle}{\langle ABi-1i \rangle \langle ABii+1 \rangle \langle ABjj+1 \rangle \langle ABj+1j+2 \rangle \langle ABm'm'+1 \rangle} \\ & + \frac{\langle ABY_4 \rangle}{\langle ABii+1 \rangle \langle ABj-1j \rangle \langle ABjj+1 \rangle \langle ABj+1j+2 \rangle \langle ABm'm'+1 \rangle} + \mathcal{R}_{c_{i+1j}} \end{aligned}$$

under the unitarity cuts of the underlined propagators, where Y_i is proportional to a line which will keep the scalar invariance of the integrand.

Proof: We transform the integrand with numerator $\langle AB\mathcal{P}_x \cap \mathcal{P}_j \rangle$ as following.

$$\begin{aligned} & \frac{\langle AB\mathcal{P}_x \cap \mathcal{P}_j \rangle}{\langle ABi-1i \rangle \langle ABii+1 \rangle \langle ABj-1j \rangle \langle ABjj+1 \rangle \langle ABj+1j+2 \rangle} \tag{4.14} \\ & = \frac{\langle ABm'm'+1 \rangle \langle AB\mathcal{P}_x \cap \mathcal{P}_j \rangle}{\langle ABi-1i \rangle \langle ABii+1 \rangle \langle ABj-1j \rangle \langle ABjj+1 \rangle \langle ABj+1j+2 \rangle \langle ABm'm'+1 \rangle} \end{aligned}$$

Then we expand the intersection of two plane as

$$\mathcal{P}_x \cap \mathcal{P}_j = a_1 L_{j-1j} + a_2 L_{jj+1} + a_3 L_{j-1j+1}, \tag{4.15}$$

where the coefficients a_i are constant which is related to the plane \mathcal{P}_x . It is obvious that only the term with line L_{j-1j+1} are not obviously of the form in (4.14). The numerator of this term is

$$\langle ABm'm'+1 \rangle \langle ABj-1j+1 \rangle. \tag{4.16}$$

Since any point in twistor space of \mathbb{CP}^3 can be expand as four independent point. Here we choose four base points $\{Z_j, Z_{i-1}, Z_i, Z_{i+1}\}$ to expand points $\{Z_{m'}Z_{m'+1}\}$. Then we can expand bi-twistor $(m'm' + 1)$ based on $(ji - 1), (ji), (ji + 1), (i - 1i), (ii + 1), (i - 1i + 1)$. Then

$$\langle ABm'm' + 1 \rangle \langle ABj - 1j + 1 \rangle \rightarrow \begin{cases} \langle ABji \rangle \langle ABj - 1j + 1 \rangle, & \langle ABji \pm 1 \rangle \langle ABj - 1j + 1 \rangle \\ & \langle ABii \pm 1 \rangle \langle ABj - 1j + 1 \rangle \\ & \langle ABi - 1i + 1 \rangle \langle ABj - 1j + 1 \rangle \end{cases}$$

According to the Schouten identity (A.7), it is easy to see that only the terms with line L_{i-1i+1} is not obvious to of the form (4.14)

$$\langle ABi - 1i + 1 \rangle \langle ABj - 1j + 1 \rangle. \quad (4.17)$$

Then expanding point Z_{j-1} as $\{Z_j, Z_{j+1}, Z_{j+2}, Z_i\}$, (4.17) can be transformed as

$$\langle ABi - 1i + 1 \rangle \langle ABj - 1j + 1 \rangle \rightarrow \begin{cases} \langle ABi - 1i + 1 \rangle \langle ABjj + 1 \rangle \\ \langle ABi - 1i + 1 \rangle \langle ABj + 2j + 1 \rangle \\ \langle ABi - 1i + 1 \rangle \langle ABij + 1 \rangle \end{cases}$$

Finally all the terms are obviously of form (4.14) according to (A.7). The integrand with numerator $\langle AB\mathcal{P}_i \cap \mathcal{P}_x \rangle$ can be also proved similarly. \square

Lemma 2 *For any unitarity cuts c_{i+1j} , we can choose a line $L_{m'} = (m'm' + 1)$ such that $\mathcal{A}_{c_{i+1j}}$ is*

$$\begin{aligned} \mathcal{A}_{c_{i+1j}} &= \mathcal{I}_5[\mathcal{P}_i \cap \mathcal{P}_j, L_{m'}] + \mathcal{I}_5[\mathcal{P}_i \cap \mathcal{P}_{j+1}, L_{m'}] \\ &+ \mathcal{I}_5[\mathcal{P}_{i+1} \cap \mathcal{P}_j, L_{m'}] + \mathcal{I}_5[\mathcal{P}_{i+1} \cap \mathcal{P}_{j+1}, L_{m'}], \end{aligned} \quad (4.18)$$

where

$$\mathcal{I}_5[\mathcal{P}_i \cap \mathcal{P}_j, L_{m'}] = \frac{\langle AB\mathcal{P}_i \cap \mathcal{P}_j \rangle \langle ijL_{m'} \rangle}{\langle ABi - 1i \rangle \langle ABii + 1 \rangle \langle ABj - 1j \rangle \langle ABjj + 1 \rangle \langle ABm'm' + 1 \rangle}.$$

The geometry of the terms are shown in Fig. 17.

Proof: According to Lemma 1, it is easy to see that the integrand (4.11) can be transformed to pentagons and boxes with one propagator $\langle ABm'm' + 1 \rangle$. The explicit

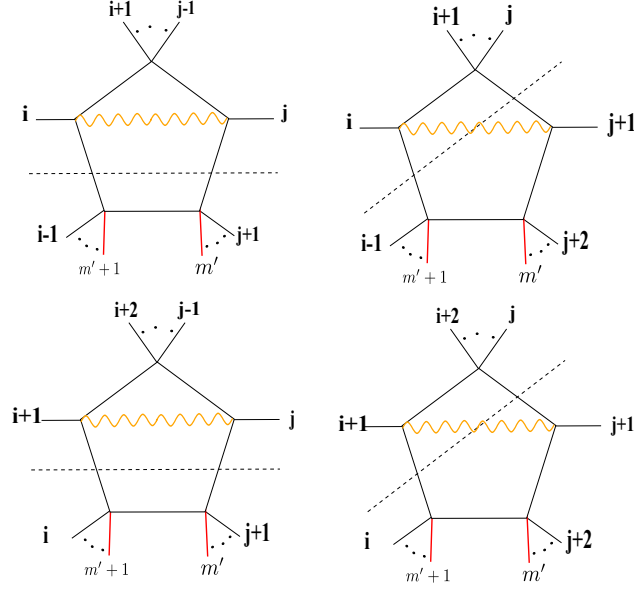


Figure 17. $\mathcal{A}_{c_{i+1j}}$ is the sum of these four terms without unphysical poles. The wavy line (ij) in this figure means the pentagon integrand $\mathcal{I}_5[\mathcal{P}_i \cap \mathcal{P}_j, (m'm' + 1)]$ and the dash line denotes the unitarity cuts.

form can be calculated directly. First, we can expand bi-twistor $(Z_{m'}Z_{m'+1})$ based on six bi-twistors in the set $\mathcal{L} = \{(Z_iZ_{i+1}), (Z_iZ_{j+1}), (Z_{i+1}Z_j), (Z_iZ_j), (Z_jZ_{j+1}), (Z_{j+1}Z_{i+1})\}$.

$$Z_{m'}Z_{m'+1} = \sum_{(Z_mZ_n) \in \mathcal{L}} \frac{\langle klm'm' + 1 \rangle}{\langle ii + 1jj + 1 \rangle} Z_mZ_n \quad (4.19)$$

where (Z_kZ_l) is the line in set \mathcal{L} which do not have the common point with (Z_mZ_n) . Then we add (Z_AZ_B) to get a $\langle ABm'm' + 1 \rangle$ as

$$\begin{aligned} \langle ABm'm' + 1 \rangle &= \frac{\langle ij + 1m'm' + 1 \rangle}{\langle ii + 1jj + 1 \rangle} \langle ABi + 1j \rangle + \frac{\langle i + 1jm'm' + 1 \rangle}{\langle ii + 1jj + 1 \rangle} \langle ABij + 1 \rangle \\ &\quad + \frac{\langle j + 1i + 1m'm' + 1 \rangle}{\langle ii + 1jj + 1 \rangle} \langle ABij \rangle + \frac{\langle ijm'm' + 1 \rangle}{\langle ii + 1jj + 1 \rangle} \langle ABj + 1i + 1 \rangle, \end{aligned} \quad (4.20)$$

where the unitarity cut condition $\langle ABii + 1 \rangle, \langle ABjj + 1 \rangle = 0$ has been applied.

Then we add term $\langle ABm'm' + 1 \rangle$ to both denominator and numerator of $\mathcal{A}_{c_{i+1j}}$, which will not affect the final answer. We first deal with the term $\mathcal{A}_{c_{i+1j}} \frac{\langle i+1jm'm'+1 \rangle}{\langle ii+1jj+1 \rangle} \frac{\langle ABij+1 \rangle}{\langle ABm'm'+1 \rangle}$. According to (4.10) and (4.11), we can get $\mathcal{A}_{c_{i+1j}} = \frac{-\langle AB(ii+1i+2) \cap (j-1jj+1) \rangle \langle ii+1jj+1 \rangle}{\langle ABii+1 \rangle \langle ABjj+1 \rangle \langle ABi+1i+2 \rangle \langle ABj-1j \rangle \langle ABj+1i \rangle}$.

Put them together, the term $\langle ABij + 1 \rangle$ vanishes, resulting

$$\begin{aligned} & \frac{\langle AB(ii + 1i + 2) \cap (j - 1jj + 1) \rangle \langle i + 1jm'm' + 1 \rangle}{\langle ABii + 1 \rangle \langle ABi + 1i + 2 \rangle \langle ABj - 1j \rangle \langle ABjj + 1 \rangle \langle ABm'm' + 1 \rangle} \\ &= \mathcal{I}_5[\mathcal{P}_{i+1} \cap \mathcal{P}_j, (m', m' + 1)], \end{aligned} \quad (4.21)$$

and this is exactly one term of the final answer. Similarly, we can get $\mathcal{I}_5[\mathcal{P}_i \cap \mathcal{P}_{j+1}, (m', m' + 1)]$ from $\frac{\langle ABi+1j \rangle}{\langle ABm'm'+1 \rangle}$. In order to get the other two terms, we need to transform as

$$\begin{aligned} \mathcal{A}_{c_{i+1j}} &= -\frac{\langle ii + 1jj + 1 \rangle^2}{\langle ABj + 1i \rangle \langle ABii + 1 \rangle \langle ABi + 1j \rangle \langle ABjj + 1 \rangle} \\ &= -\frac{\langle ii + 1jj + 1 \rangle^2}{\langle ABii + 1 \rangle \langle ABjj + 1 \rangle \langle ABj + 1i + 1 \rangle \langle ABij \rangle} \end{aligned} \quad (4.22)$$

based on Schouten identity and unitarity cut condition. Also, use the relation between dash line and wavy line, we can get

$$\frac{\langle ii + 1jj + 1 \rangle}{\langle ABij \rangle} = -\frac{\langle AB(i - 1ii + 1) \cap (j - 1jj + 1) \rangle}{\langle ABi - 1i \rangle \langle ABj - 1j \rangle} \quad (4.23)$$

if we use this equation to replace $\langle ABij \rangle$, while the remaining $\langle ABj + 1i + 1 \rangle$ will be canceled by terms in $\langle ABm'm' + 1 \rangle$, and will become $\mathcal{I}_5[\mathcal{P}_i \cap \mathcal{P}_j, (m', m' + 1)]$ \square

Lemma 3 *Under the unitarity cut c_{i+1n-1} we have*

$$\begin{aligned} & \mathcal{I}_5[\mathcal{P}_j \cap \mathcal{P}_i, (n - 1n)] + \mathcal{I}_5[\mathcal{P}_j \cap \mathcal{P}_{i+1}, (n - 1n)] \\ &= \mathcal{H}_{j-1j} - \mathcal{H}_{jj+1} + \mathcal{R}_{c_{i+1n-1}}, \end{aligned} \quad (4.24)$$

where

$$\begin{aligned} \mathcal{H}_{j-1j} &= \frac{\langle j - 1j(ABn - 1) \cap \mathcal{P}_i \rangle \langle ii + 1i + 2n \rangle}{\langle ABj - 1j \rangle \langle ABi - 1i \rangle \langle ABii + 1 \rangle \langle ABi + 1i + 2 \rangle \langle ABn - 1n \rangle} \\ &+ \frac{\langle j - 1j(ABn) \cap \mathcal{P}_i \rangle \langle n - 1ii + 1i + 2 \rangle}{\langle ABj - 1j \rangle \langle ABi - 1i \rangle \langle ABii + 1 \rangle \langle ABi + 1i + 2 \rangle \langle ABn - 1n \rangle}. \end{aligned} \quad (4.25)$$

Proof: First we expand $\langle AB\mathcal{P}_j \cap \mathcal{P}_{i+1} \rangle$ and add a term $\langle ABi - 1i \rangle$ both in the numerator and denominator. Since two parts have the same denominator, we only deal with the numerators. We first deal with $\langle AB\mathcal{P}_j \cap \mathcal{P}_{i+1} \rangle \langle ABi - 1i \rangle$

$$\begin{aligned} & \langle AB\mathcal{P}_j \cap \mathcal{P}_{i+1} \rangle \\ &= \langle ABj - 1j \rangle \langle j + 1ii + 1i + 2 \rangle + \langle ABjj + 1 \rangle \langle j - 1ii + 1i + 2 \rangle + \langle ABj - 1j + 1 \rangle \langle ii + 1i + 2j \rangle. \end{aligned}$$

We expand Z_{i-1} in $\langle ABi - 1i \rangle$ based on Schouten identity in each term in previous equation and obtain six terms. The sum of three terms which have the same factor $\langle i - 1ii + 1i + 2 \rangle$ is $\langle i - 1ii + 1i + 2 \rangle (\langle ABj - 1j \rangle \langle ABj + 1i \rangle + \langle ABjj + 1 \rangle \langle ABj - 1i \rangle - \langle ABj - 1j + 1 \rangle \langle ABji \rangle)$. Three terms in the bracket equals zero based on Schouten identity. And the sum of remaining terms forms $\langle AB\mathcal{P}_j \cap \mathcal{P}_i \rangle \langle ABi + 2i \rangle$. Now we can get an very important equation

$$\langle AB\mathcal{P}_j \cap \mathcal{P}_{i+1} \rangle \langle ABi - 1i \rangle = \langle AB\mathcal{P}_j \cap \mathcal{P}_i \rangle \langle ABi + 2i \rangle \quad (4.26)$$

The sum of the two numerators in (4.24) is

$$\langle AB\mathcal{P}_j \cap \mathcal{P}_i \rangle (\langle ABi + 2i \rangle \langle ji + 1n - 1n \rangle + \langle ABi + 1i + 2 \rangle \langle jin - 1n \rangle) \quad (4.27)$$

Now we deal with $(\langle ABi + 2i \rangle \langle ji + 1n - 1n \rangle + \langle ABi + 1i + 2 \rangle \langle jin - 1n \rangle)$

$$\begin{aligned} & \langle ABi + 2i \rangle \langle ji + 1n - 1n \rangle + \langle ABi + 1i + 2 \rangle \langle jin - 1n \rangle \quad (4.28) \\ &= \langle ii + 1(ABi + 2) \cap (jn - 1n) \rangle \\ &= \langle ii + 1Bi + 2 \rangle \langle Ajn - 1n \rangle + \langle ii + 1Ai + 2 \rangle \langle jn - 1nB \rangle \\ &= \langle BA(ii + 1i + 2) \cap (jn - 1n) \rangle \\ &= \langle ABn - 1j \rangle \langle ii + 1i + 2n \rangle + \langle ABnj \rangle \langle n - 1ii + 1i + 2 \rangle, \end{aligned}$$

where unitarity condition related to $\langle ABii + 1 \rangle$ and $\langle ABn - 1n \rangle$ has been applied. There will be three terms related to $\langle ABj - 1j \rangle$, $\langle ABjj + 1 \rangle$ and $\langle ABj - 1j + 1 \rangle$ in $\langle AB\mathcal{P}_j \cap \mathcal{P}_i \rangle$. However, according to $\langle ABj - 1j + 1 \rangle \langle ABkj \rangle = \langle ABj - 1k \rangle \langle ABj + 1j \rangle + \langle ABj - 1j \rangle \langle ABkj + 1 \rangle$ (Z_k could be any twistor), (4.27) only have two terms related to $\langle ABj - 1j \rangle$, $\langle ABjj + 1 \rangle$. The sum of terms contain $\langle ABj - 1j \rangle$ is

$$\begin{aligned} & (\langle ABn - 1j \rangle \langle ii + 1i + 2n \rangle \langle j + 1i - 1ii + 1 \rangle \\ &+ \langle ABnj \rangle \langle n - 1ii + 1i + 2 \rangle \langle j + 1i - 1ii + 1 \rangle \\ &+ \langle ABn - 1j + 1 \rangle \langle ii + 1i + 2n \rangle \langle i - 1ii + 1j \rangle \\ &+ \langle ABnj + 1 \rangle \langle n - 1ii + 1i + 2 \rangle \langle i - 1ii + 1j \rangle) \langle ABj - 1j \rangle \\ &= (\langle j + 1j(ABn - 1) \cap (i - 1ii + 1) \rangle \langle ii + 1i + 2n \rangle \\ &+ \langle j + 1j(ABn) \cap (i - 1ii + 1) \rangle \langle n - 1ii + 1i + 2 \rangle) \langle ABj - 1j \rangle. \quad (4.29) \end{aligned}$$

Similarly, we can get $\langle ABjj + 1 \rangle (\langle j - 1j(ABn - 1) \cap (i - 1ii + 1) \rangle \langle ii + 1i + 2n \rangle + \langle j - 1j(ABn) \cap (i - 1ii + 1) \rangle \langle n - 1ii + 1i + 2 \rangle)$. Combine numerator and denominator, we can get $\mathcal{H}_{j-1j} - \mathcal{H}_{jj+1}$. \square

Lemma 4 *The integrand $\mathcal{A}_{c_{i+1n-1}}$ is equal to the integrand $\mathcal{A}_{C_{1n-2}}$ with reference line L_{n-1} under unitarity cut c_{i+1n-1} .*

Proof: First we find out the terms in $\mathcal{A}_{C_{1n-2}}$ which contain both $\langle ABi+1 \rangle$ and $\langle ABn-1n \rangle$. We need to prove

$$\begin{aligned} \mathcal{A}_{c_{i+1n-1}} &= \sum_{j=1}^{i-1} (\mathcal{I}_5[\mathcal{P}_j \cap \mathcal{P}_i, (n-1n)] + \mathcal{I}_5[\mathcal{P}_j \cap \mathcal{P}_{i+1}, (n-1n)]) \\ &+ \sum_{j=i+2}^{n-2} (\mathcal{I}_5[\mathcal{P}_j \cap \mathcal{P}_i, (n-1n)] + \mathcal{I}_5[\mathcal{P}_j \cap \mathcal{P}_{i+1}, (n-1n)]) \\ &+ \mathcal{I}_5[\mathcal{P}_i \cap \mathcal{P}_{i+1}, (n-1n)] \end{aligned} \quad (4.30)$$

According to Lemma 3, term $-\mathcal{H}_{jj+1}$ in $(\mathcal{I}_5[\mathcal{P}_j \cap \mathcal{P}_i, (n-1n)] + \mathcal{I}_5[\mathcal{P}_j \cap \mathcal{P}_{i+1}, (n-1n)])$ will be canceled by terms of \mathcal{H}_{jj+1} in $(\mathcal{I}_5[\mathcal{P}_{j+1} \cap \mathcal{P}_i, (n-1n)] + \mathcal{I}_5[\mathcal{P}_{j+1} \cap \mathcal{P}_{i+1}, (n-1n)])$. After sum over all possible terms of c_{i+1n-1} , only four terms left

$$\mathcal{A}_{c_{i+1n-1}} = \mathcal{H}_{(n1)} - \mathcal{H}_{(i-1i)} + \mathcal{H}_{(i+1i+2)} - \mathcal{H}_{(n-2n-1)} + \mathcal{I}_5[\mathcal{P}_i \cap \mathcal{P}_{i+1}, (n-1n)]. \quad (4.31)$$

For every term in previous equation,

$$\begin{aligned} \mathcal{H}_{n1} &= \mathcal{I}_5[\mathcal{P}_{i+1} \cap \mathcal{P}_n, (i-1i)] \\ \mathcal{H}_{i-1i} &= 0 \\ \mathcal{H}_{i+1i+2} &= -\mathcal{I}_5[\mathcal{P}_i \cap \mathcal{P}_{i+1}, (n-1n)] \\ \mathcal{H}_{n-2n-1} &= -\mathcal{I}_5[\mathcal{P}_{i+1} \cap \mathcal{P}_{n-1}, (i-1i)] \end{aligned} \quad (4.32)$$

So

$$\mathcal{A}_{c_{i+1n-1}} = \mathcal{I}_5[\mathcal{P}_{i+1} \cap \mathcal{P}_n, (i-1i)] + \mathcal{I}_5[\mathcal{P}_{i+1} \cap \mathcal{P}_{n-1}, (i-1i)] \quad (4.33)$$

This result is the same as $\mathcal{A}_{c_{i+1n-1}}$ in Lemma 2, if we pick $(Z_{m'}Z_{m'+1}) = (Z_{i-1}Z_i)$. \square

Theorem 1 *The integrand of MHV one loop amplitudes can be constructed by the union over all the integrand from each unitarity cut. If we choose the reference line to be L_{n-1} , the integrand of MHV one loop amplitudes is*

$$\mathcal{A}_{C_{1n}} = \mathcal{A}_{C_{1n-2}} = \bigcup_{1 \leq i < j < n-1} \mathcal{A}_{c_{ij}} = \sum_{1 \leq i < j < n-1} \mathcal{I}_5[\mathcal{P}_i \cap \mathcal{P}_j, L_{n-1}] \quad (4.34)$$

Proof: As discuss above, for convenience, we unite the $\mathcal{A}_{c_{ij}}$ in a union order. In general, when uniting integrands $\mathcal{A}_{c_{i-1j}}$ and $\mathcal{A}_{C_{ij}}$, the only cut-related terms in $\mathcal{A}_{C_{ij}}$ which may influence the unitarity cuts of c_{i-1j} are $\{c_{i-1j-1}, c_{ij}, c_{ij-1}\}$. On the other hand, $\mathcal{A}_{c_{i-1j}}$ may affect the cuts $\{c_{i-1j-1}, c_{ij}, c_{ij-1}\}$ in C_{ij} . Hence we only need verify that the cut-related terms in $\mathcal{A}_{C_{ij}}$ are either same with the terms in $\mathcal{A}_{c_{i-1j}}$ or cut un-related with each other. This is easy to prove according to Lemma 2. Hence we can unite over all the terms except the last column in 1. According the Lemma 4, we do not need to unite over the integrand from the last column and the union of C_{1n-2} is just the final integrand from the unitarity cuts up to a rational function on all the unitarity cuts. We find such construction of integrand is equivalent to the integrand from single cuts in [21, 22]. \square

4.2 MHV nonplanar amplitudes and unitarity cuts

In this section, we will present a general recipe for dealing with MHV nonplanar amplitudes. One-loop four-point and five-point amplitudes are carefully worked out as examples.

Properties of MHV nonplanar amplitudes under unitarity cuts

We consider first the situation with only one nonplanar leg. Based on the permutation relations of Yangian Invariants (2.1) this amplitude under a unitarity cut can be converted to a planar one at a price of a simple factor f_{kin} in Fig. 18

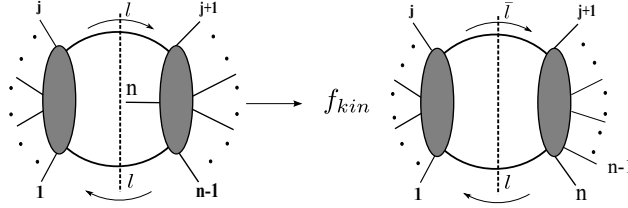


Figure 18. A nonplanar one-loop n -point MHV amplitude, with one nonplanar leg marked “ n ”, can be converted to a planar one at the price of a simple kinematic factor f_{kin} .

$$f_{kin} = \frac{\langle n-1n \rangle \langle \bar{l} \rangle}{\langle n-1l \rangle \langle n\bar{l} \rangle}. \quad (4.35)$$

This step removes one nonplanar leg. For more than one nonplanar legs, say m , we can repeat this operation m times to arrive at a planar diagram. Planar MHV amplitudes

under unitarity cuts have been discussed in section 4.1 we can therefore apply the planar results to obtain the nonplanar MHV amplitude after a unitarity cut by

$$A_c(1, 2, \dots, j | j+1, \dots, n-1, \dot{n}) = f_{kin} A_c(1, j | j+1, n), \quad (4.36)$$

where ‘ \dot{i} ’ labels the nonplanar leg and A is planar if there is no dotted leg in the arguments. This equation clearly shows that the difference between the planar result and the nonplanar one lies in the kinematic factors.

Reconstructing the kinematic factors:

Amplitudes under a unitarity cut only contains two variables related to the loop momentum. Unitarity cut condition sets two cut propagators to zero, while fixing the other two variables. With this in mind we need to reconstruct the amplitudes to a function of four variables. A unitarity cut on nonplanar diagrams contains two pieces of information, the kinematic factor and the corresponding planar amplitudes. We need to discuss them separately. As reconstruction of planar part is the same as above we deal with the kinematic factors here.

For one nonplanar leg (labelled n), we can read off from Fig. 18 the kinematic factor as

$$f_{kin} = \frac{\langle n-1n \rangle \langle \bar{l}l \rangle}{\langle n-1l \rangle \langle n\bar{l} \rangle} \quad (4.37)$$

Using Schouten identity, and expanding spinor λ_{n-1} based on λ_{j+1} and λ_n as

$$\lambda_{n-1} = \frac{\langle n-1, n \rangle}{\langle j+1, n \rangle} \lambda_{j+1} + \frac{\langle j+1, n-1 \rangle}{\langle j+1, n \rangle} \lambda_n,$$

f_{kin} can be expanded as

$$f_{kin} = -1 + \frac{\langle ln \rangle \langle \bar{l}j+1 \rangle \langle n-1, n \rangle}{\langle ln-1 \rangle \langle \bar{l}n \rangle \langle j+1, n \rangle} + \frac{\langle ln \rangle \langle j+1, n-1 \rangle}{\langle l, n-1 \rangle \langle j+1, n \rangle}. \quad (4.38)$$

Under a unitarity cut, variables l and \bar{l} in momentum space are denoted by variables A and B in momentum twistor space. So $\langle ln \rangle \langle \bar{l}j+1 \rangle$ can be rewritten as $\langle An \rangle \langle Bj+1 \rangle$. Using the equation

$$\langle ABi-1i \rangle = \langle AB \rangle \langle i-1i \rangle (x-x_i)^2$$

we express f_{kin} as

$$f_{kin} = -1 + \frac{\langle AnBj+1 \rangle^{o1} \langle n-1n \rangle}{\langle An-1Bn \rangle^{o2} \langle j+1n \rangle} + \frac{\langle AnBj+1 \rangle^{o1} \langle j+1n-1 \rangle}{\langle An-1Bj+1 \rangle^{o3} \langle j+1n \rangle} \quad (4.39)$$

We take a pause here to clarify our notations. The expansion of $\langle ABi-1i \rangle$ is valid if A and B , $i-1$ and i are continuous in a certain color ordering in twistor space. Now A and $n-1$, and B and n are in fact not continuous in the original color ordering. We can, nevertheless, define a new color ordering, labeled by $o2$ in equation, where in this ordering A and $n-1$, and B and n are both continuous. In addition if we choose

$$\begin{aligned} o1 &= (1, 2, \dots, j, j+1, \dots, n) \\ o2 &= (1, 2, \dots, j, n, \dots, n-1) \\ o3 &= (1, 2, \dots, j, j+1, \dots, n, n-1) \end{aligned}$$

then $(p_A + p_B)^2$ will appear both in the denominator and numerator and cancel each other. Thus the former equation (4.39) is naturally true.

The next step is to combine kinematic factors with the planar amplitudes. Recall that the planar amplitudes

$$\begin{aligned} &\mathcal{A}_0(1, \dots, j|j+1, \dots, n) \\ &= \mathcal{A}_n^{tree_{MHV}} \cdot \frac{-\langle j+1ii+1j \rangle^2}{\langle ABj+1i \rangle \langle ABii+1 \rangle \langle ABi+1j \rangle \langle ABjj+1 \rangle} \end{aligned} \quad (4.40)$$

(Here we add the MHV tree amplitudes as a coefficient because, in nonplanar situation, this coefficient is important and can not be omitted). It is then clear that the numerator $\langle AnBj+1 \rangle^{o1}$ will cancel the same term in the denominator of $\mathcal{A}_0(1, 2, \dots, j|j+1, \dots, n)$ by adding a new term related to $o2$ or $o3$, and consequently changing the color ordering. Hence

$$\begin{aligned} &f_{kin} \mathcal{A}_0(1, \dots, j|j+1, \dots, n) \\ &= -\mathcal{A}_0(1, \dots, j|j+1, \dots, n) - \mathcal{A}_0(1, \dots, j|n, \dots, n-1) \\ &\quad - \frac{\langle nn-2 \rangle \langle n-1j+1 \rangle}{\langle n-2n-1 \rangle \langle nj+1 \rangle} \cdot \mathcal{A}_0(1, \dots, j|j+1, \dots, n-1) \end{aligned} \quad (4.41)$$

This is nothing but \mathcal{A}_0 with unphysical poles, which needs to be converted to \mathcal{A}_1 , which only contains physical poles, to arrive at the final results. This can be achieved in a way completely analogous to the procedures presented in Section 4.1.

Comparison with $U(1)$ decoupling relation

As alluded above a relation of reconstructed amplitudes from permutation relation of Yangian Invariants has only these three terms (or two terms in the case of four-point).

$$\begin{aligned}
& \mathcal{A}_1(1, 2, \dots, j|j+1, \dots, n-1, \dot{n}) \\
&= f_{kin} \mathcal{A}_1(1, 2, \dots, j|j+1, \dots, n) \\
&= -\mathcal{A}_1(1, 2, \dots, j|j+1, \dots, n) - \mathcal{A}_1(1, 2, \dots, j|n, \dots, n-1) \\
&\quad - \frac{\langle n n-2 \rangle \langle n-1 j+1 \rangle}{\langle n-2 n-1 \rangle \langle n j+1 \rangle} \cdot \mathcal{A}_1(1, 2, \dots, j|j+1, \dots, n, n-1)
\end{aligned}$$

When considering the $U(1)$ decoupling relation

$$\begin{aligned}
& \mathcal{A}_1(1, 2, \dots, j|j+1, \dots, n-1, \dot{n}) \\
&= -\mathcal{A}_1(1, 2, \dots, j|j+1, \dots, n) - \mathcal{A}_1(1, 2, \dots, j|n, \dots, n-1) \\
&\quad - \sum_i \mathcal{A}_1(1, 2, \dots, j|j+1, \dots, i, n, i+1, \dots, n-1), \tag{4.42}
\end{aligned}$$

more terms will appear. However, due to the special property of MHV amplitudes, the exchange of external legs which are not the four legs connecting the “basic twin-box” will not affect the final result of this cut. That is to say, all of the possible cases in this set have the same cut amplitudes. The only difference is the pre-factor, MHV tree amplitude. If we expand the factor

$$\frac{\langle n n-2 \rangle \langle n-1 j+1 \rangle}{\langle n-2 n-1 \rangle \langle n j+1 \rangle}$$

we can find cuts with all possible color ordering, which are the same as obtained from $U(1)$ decoupling. This form is obviously more compact than $U(1)$ decoupling, since it combines, in one integral, terms related to planar amplitudes of different orders but having same result under a given unitarity cut.

Final results of MHV nonplanar amplitudes:

Final results of MHV nonplanar amplitudes are the union of all possible $f_{kin} \mathcal{A}_1$

$$\mathcal{A}_{NP} = \bigcup_i f_{kin}^i \mathcal{A}_{1i} \tag{4.43}$$

where \mathcal{A}_{NP} stands for the final results of nonplanar amplitudes and \mathcal{A}_P is the final results of planar counterparts.

This formula just give a procedure, which is the same as the planar situation, to get the final result. However, to get the general formula of integrand, a lemma needs to

be proved. When two terms in two different cut results are cut related (one term has propagators of the other unitarity cuts), one of them can convert to terms which are the same as the other one and others that are cut un-related. We will prove it in future work. In the following sections, we will show this method is valid in some particular examples of four-point and five-point situation.

4.3 One-loop four-point MHV nonplanar amplitudes

In this section we describe a nonplanar four point amplitude with one nonplanar leg (we call “(3+1)” case) as an explicit example of our construction.

We start with the cut result of this case, which is shown in Fig. 10. First, we convert this cut amplitude to planar one with a kinematic factor. in Fig. 19.

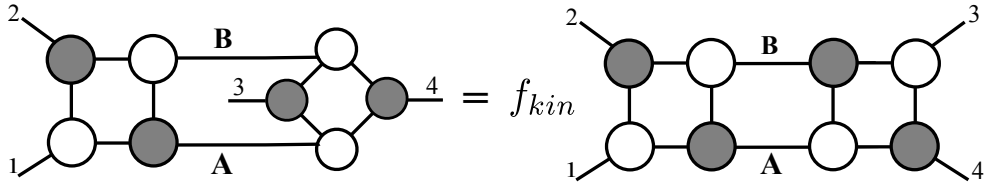


Figure 19. Convert the nonplanar cut amplitude to planar one with a kinematic factor

The way to reconstruct the planar diagram is simply adding two BCFW bridges across legs (2 3) and (1 4). The result is exactly the one loop four-point planar amplitude 20. We can simply write down the result of the diagram above in the form of loop

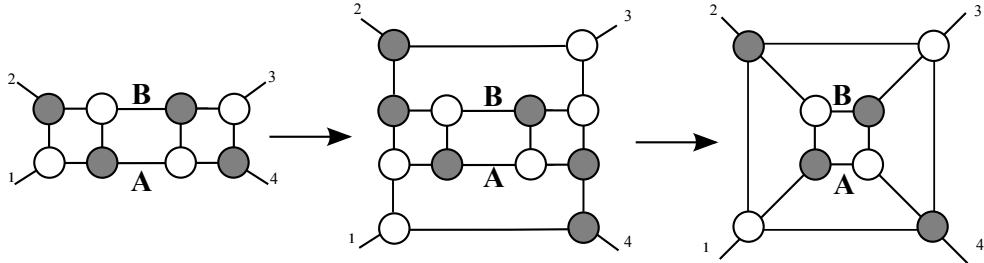


Figure 20. Way of reconstruct the planar diagram. First step is adding two BCFW bridges. Using “square moves” and “merges” to represent the diagram as shown in [35].

integrand.

$$\mathcal{A}_0(1, 2, 3, 4) = \frac{-\langle 1234 \rangle^2}{\langle AB12 \rangle \langle AB23 \rangle \langle AB34 \rangle \langle AB41 \rangle} \quad (4.44)$$

Here $\mathcal{A}_0 = \mathcal{A}_1$ because there are only four points, we need not to remove unphysical poles.

Using the unitarity cut condition $\langle AB23 \rangle = 0, \langle AB41 \rangle = 0$, we can rewrite the kinematic factor as

$$f_{kin} = \frac{s_{l_2}}{s_{l_3}} = -1 - \frac{\langle AB34 \rangle^{o1}}{\langle AB43 \rangle^{o2}}$$

Here we define two color orders, o^1 means color order (1,2,3,4), and o^2 means (1,2,4,3). Combine the factor and planar result, we can get

$$\begin{aligned} & \mathcal{A}_1(1, 2|3, \dot{4}) \\ &= \mathcal{A}_4^{MHVtree}(1, 2, 3, 4) \left(1 + \frac{\langle AB34 \rangle^{o1}}{\langle AB43 \rangle^{o2}}\right) \frac{\langle 1234 \rangle^2}{\langle AB12 \rangle \langle AB23 \rangle \langle AB34 \rangle \langle AB41 \rangle} \\ &= \mathcal{A}_4^{MHVtree}(1, 2, 3, 4) \frac{\langle 1234 \rangle^2}{\langle AB12 \rangle^{o1} \langle AB23 \rangle^{o1} \langle AB34 \rangle^{o1} \langle AB41 \rangle^{o1}} \\ & \quad + \mathcal{A}_4^{MHVtree}(1, 2, 4, 3) \frac{\langle 1243 \rangle^2}{\langle AB12 \rangle^{o2} \langle AB24 \rangle^{o2} \langle AB43 \rangle^{o2} \langle AB31 \rangle^{o2}} \end{aligned} \quad (4.45)$$

Other possible unitarity cuts should be taken into consideration. The steps to deal with all possible unitarity cuts are as described above. Since each term is actually the planar four-point one-loop amplitude with a certain color ordering, we can simplify the expression as

$$\begin{aligned} \mathcal{A}_1(1, 2|3, \dot{4}) &= \mathcal{A}_P(1, 2, 3, 4) + \mathcal{A}_P(1, 2, 4, 3) \\ \mathcal{A}_1(2, 3|1, \dot{4}) &= \mathcal{A}_P(2, 3, 1, 4) + \mathcal{A}_P(2, 3, 4, 1) \\ \mathcal{A}_1(3, 1|2, \dot{4}) &= \mathcal{A}_P(3, 1, 2, 4) + \mathcal{A}_P(3, 1, 4, 2) \end{aligned}$$

Now we need to unite $\mathcal{A}_1(2, 3|1, \dot{4})$ and $\mathcal{A}_1(1, 2|3, \dot{4})$. Obviously, the terms with $o1$ are the same in these two. While it is not obvious to judge whether other terms are cut related or not. However, we can set one of the cut propagator in all terms as l^2 in momentum space and write down the denominators of these three terms.

$$\begin{aligned} o1(1, 2, 3, 4) &: \frac{l^2(l-p_1)^2(l-p_1-p_2)^2(l+p_4)^2}{\langle AB12 \rangle \langle AB23 \rangle \langle AB34 \rangle \langle AB41 \rangle} \\ o2(1, 2, 4, 3) &: \frac{l^2(l-p_1)^2(l-p_1-p_2)^2(l+p_3)^2}{\langle AB12 \rangle \langle AB24 \rangle \langle AB43 \rangle \langle AB31 \rangle} \\ o3(2, 3, 1, 4) &: \frac{l^2(l-p_1)^2(l-p_1-p_4)^2(l+p_3)^2}{\langle AB23 \rangle \langle AB31 \rangle \langle AB14 \rangle \langle AB42 \rangle} \end{aligned} \quad (4.46)$$

Now we can clearly find out that the terms of $o3$ in $\mathcal{A}_1(2, 3|1, \dot{4})$ do not have common unitarity cuts with the terms in $\mathcal{A}_1(1, 2|3, \dot{4})$ and vice versa. So, according to the

definition of operation union,

$$\mathcal{A}_1(1, 2|3, \dot{4}) \cup \mathcal{A}_1(2, 3|1, \dot{4}) = \mathcal{A}_P(1, 2, 3, 4) + \mathcal{A}_P(1, 2, 4, 3) + \mathcal{A}_P(3, 1, 2, 4). \quad (4.47)$$

So we can obtain the final result of nonplanar amplitude as

$$\begin{aligned} \mathcal{A}_{NP}(1, 2, 3, \dot{4}) &= \bigcup_{i=1}^3 (\mathcal{A}_{NP}(i, i+1|i+2, \dot{4})) \\ &= \mathcal{A}_P(1, 2, 3, 4) + \mathcal{A}_P(1, 2, 4, 3) + \mathcal{A}_P(1, 4, 2, 3), \end{aligned} \quad (4.48)$$

which is the familiar result of nonplanar “(3+1)” case [5].

4.4 One-loop five-point MHV nonplanar amplitudes

We first obtain all the unitarity cuts of five point nonplanar amplitudes $A_c(1, 2, 3, 4, \dot{5})$ as following

Cut Type I

$$A_c(1, \dot{5}|2, 3, 4), A_c(2, \dot{5}|3, 4, 1), A_c(3, \dot{5}|2, 4, 1), A_c(4, \dot{5}|3, 2, 1)$$

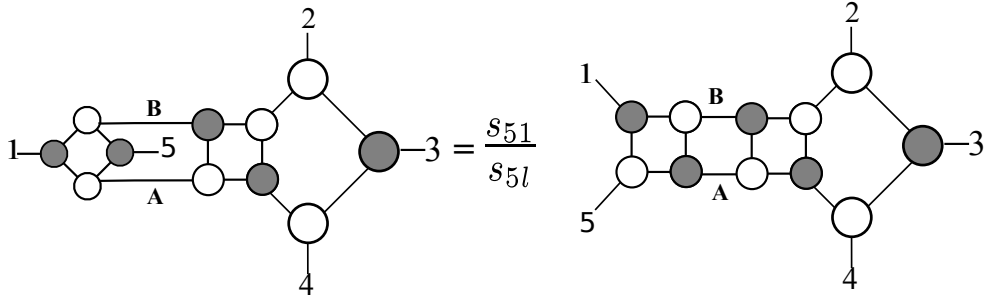


Figure 21. On-shell diagram of cut amplitude $\mathcal{A}_c(1, \dot{5}|2, 3, 4)$

Cut Type II

$$A_c(1, 2|3, 4, \dot{5}), A_c(1, 2, \dot{5}|3, 4), A_c(2, 3|4, 1, \dot{5}), A_c(2, 3, \dot{5}|4, 1).$$

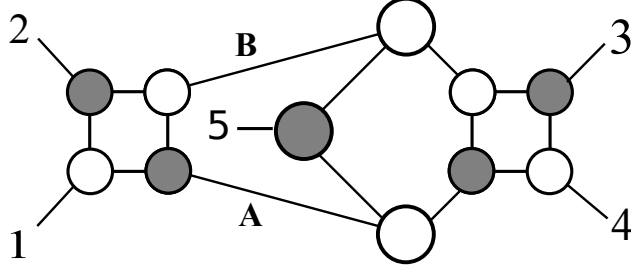


Figure 22. On-shell diagram of cut amplitude $\mathcal{A}_c(1, 2|3, 4, \dot{5})$

For the Cut Type I, the tree level part of nonplanar leg is four point amplitude. While for the Cut Type II, the tree level part of nonplanar leg is five point amplitude. In both cases, all the tree part under a unitarity cut are MHV amplitudes.

Since case I are actually the same situation as the four-point ones, we just simply write down the result.

$$\begin{aligned}
 A_c(1, \dot{5}|2, 3, 4) &= \frac{s_{15}}{s_{t5}} A_c(51|234) \\
 \mathcal{A}_1(1, \dot{5}|2, 3, 4) &= \mathcal{A}_1(1, 5|2, 3, 4) + \mathcal{A}_1(5, 1|2, 3, 4)
 \end{aligned}
 \tag{4.49}$$

For case II, take $\mathcal{A}_c(1, 2|3, 4, \dot{5})$ as an example, we can get the relation in bipartite on-shell diagram as Fig. 23

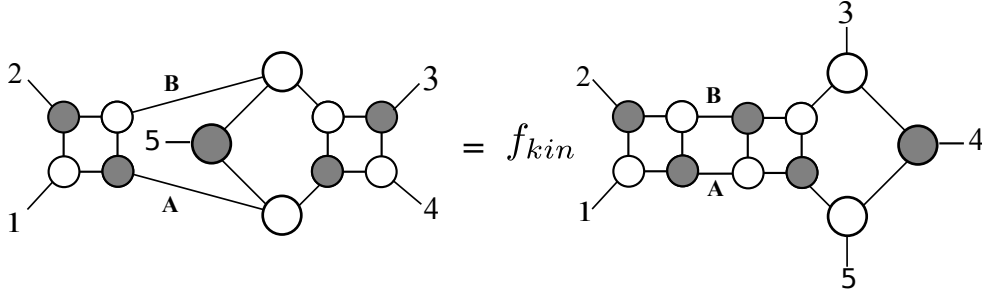


Figure 23. Permutation relation in $\mathcal{A}_c(1, 2|3, 4, \dot{5})$

The planar part can be done with the same strategy above, and covert to box integrand. Here we first deal with the kinematic factor $f_{kin} = \frac{\langle 45 \rangle \langle \bar{l} \bar{l} \rangle}{\langle l4 \rangle \langle \bar{l} 5 \rangle}$

Considering different color order, we can get

$$f_{kin} = -1 + \frac{\langle A5B3 \rangle^{o1} \langle 45 \rangle}{\langle A4B5 \rangle^{o2} \langle 35 \rangle} + \frac{\langle A5B3 \rangle^{o1} \langle 34 \rangle}{\langle A4B3 \rangle^{o3} \langle 35 \rangle}
 \tag{4.50}$$

Then we can simply write

$$\mathcal{A}_0(1, 2|3, 4, 5) = \mathcal{A}_5^{treeMHV} \frac{-\langle 1235 \rangle^2}{\langle AB12 \rangle \langle AB23 \rangle \langle AB35 \rangle \langle AB51 \rangle}.$$

Combining f_{kin} and $\mathcal{A}_0(1, 2|3, 4, 5)$ we get

$$\begin{aligned} \mathcal{A}_0(1, 2|3, 4, \dot{5}) &= f_{kin} \mathcal{A}_0(1, 2|3, 4, 5) \\ &= -(\mathcal{A}_0(1, 2|3, 4, 5) + \mathcal{A}_0(1, 2|3, 5, 4) + \mathcal{A}_0(1, 2|5, 3, 4)) \end{aligned} \quad (4.51)$$

Upon eliminating unphysical poles \mathcal{A}_1 becomes

$$\mathcal{A}_1(1, 2|3, 4, 5) = \frac{\langle AB(234) \cap (451) \rangle \langle 3512 \rangle}{\langle AB12 \rangle \langle AB23 \rangle \langle AB34 \rangle \langle AB45 \rangle \langle AB51 \rangle} \quad (4.52)$$

Uniting $\mathcal{A}_1(1, 2|3, 4, \dot{5})$ and $\mathcal{A}_1(2, 3|4, 1, \dot{5})$ based on the same method in four-point case, we can find that every term is only cut-related with the results of its own color order, while not affect those of other orders under unitary cuts. The final non-planar integrand is the union of all five cuts,

$$\mathcal{A}_{NP}(1, 2, 3, 4, \dot{5}) = \bigcup_i f_{kin}^i \mathcal{A}_1(i, i+1|i+2, i+3, \dot{5}). \quad (4.53)$$

This result contains all of the possible results of unitary cuts in all possible color orders $(i, i+1, i+2, i+3, 5), i = 1, 2, 3, 4$ of planar amplitudes. For instance, we can find all unitary cuts $\mathcal{A}_1(i, i+1|i+2, i+3, i+4), i = 1, 2, 3, 4, 5$ of order $(1, 2, 3, 4, 5)$. According to the discussion in planar MHV amplitudes, the union of these cuts can get $\mathcal{A}_P(1, 2, 3, 4, 5)$. In the same way, we can get $\mathcal{A}_P(1, 2, 3, 5, 4)$, $\mathcal{A}_P(1, 2, 5, 3, 4)$, $\mathcal{A}_P(1, 5, 2, 3, 4)$. Since results from different orders do not affect each other under unitary cuts, the union of all non-planar results equals to the sum of the unions of every order

$$\mathcal{A}_{NP}(1234\dot{5}) = \mathcal{A}_P(12345) + \mathcal{A}_P(12354) + \mathcal{A}_P(12534) + \mathcal{A}_P(15234). \quad (4.54)$$

5 NMHV nonplanar amplitude from double unitarity cuts

In this section we will present results of a 6-point one loop NMHV nonplanar amplitude, by double unitarity cuts, in the invariant top form. It is convenient to see the geometric structures of the amplitudes from this invariant top form [35]. In order to write the

total amplitude in the top form the newly found permutation relation of the Yangian Invariants again comes in handy.

Before investigating specific examples we propose the general procedures of constructing total amplitudes for one loop nonplanar Feynman diagrams. At one loop level the planar diagrams corresponds to the single-trace partial amplitudes in color-order decomposition. The planar on-shell diagrams are associated with the $(k \times n)$ Grassmannian Matrices [35], C ,

$$C = \begin{pmatrix} c_{11} & c_{12} & \cdots & c_{1n} \\ c_{21} & c_{22} & \cdots & c_{2n} \\ \vdots & \vdots & \ddots & \vdots \\ c_{k1} & c_{k2} & \cdots & c_{kn} \end{pmatrix} \quad (5.1)$$

It is of convenience to view the Grassmannian cell C as a collection of k -dimensional columns $\{\vec{c}_1, \vec{c}_2 \cdots \vec{c}_n\}$. There are $k \times (n-k)$ parameter for a generic Grassmannian matrix C , of which $2n - 4$ parameter are determined by the δ -functions $\delta(C \cdot \vec{\lambda})$ and $\delta(\vec{\lambda} \cdot C^\perp)$ in (2.13) and others are determined by the linear-structures of the on-shell reduced diagrams. As discussed in [35], for planar diagrams, such linear-structures of linear-dependencies among consecutive chains of columns is known as positroid stratification [53, 54]. The top form of correct singularities should be

$$\Omega = \frac{d^{k \times n} C}{\text{vol}(GL(k))} \frac{1}{(1 \cdots k) \cdots (n \cdots k - 1)}, \quad (5.2)$$

where $(1 \cdots k)$ is the minor of matrix $\{\vec{c}_1 \cdots \vec{c}_k\}$. Hence the top forms of planar diagrams are characterized by consecutive minors of the Grassmannian matrix.

Corresponding to double-trace partial amplitudes, every on-shell bipartite diagram of the leading singularity in a double-trace partial amplitudes is also associated with Grassmannian cell $C^{k \times n} = \{\vec{c}_1, \cdots, \vec{c}_j, \vec{c}_{j+1} \cdots \vec{c}_n\}$. And C are determined by the δ -function in (2.13) and the linear-structures of the on-shell reduced diagrams. Since such nonplanar diagrams are endowed with two cyclic-orderings for $\{\vec{c}_1, \cdots, \vec{c}_j\}$ and $\{\vec{c}_{j+1} \cdots \vec{c}_n\}$ respectively. By hunch, the linear-structures is the linear-dependencies among the chains of columns with consecutive legs with respect to each cyclic-ordering, and hence is a stratification of $G(k, n)$. Since the linear-dependencies are characterized by the minors. The external leg indexes of the columns in each minor, if they are in the same trace, should be consecutive. Hence the proper minors are

$$\mathcal{M} = \{(1 \cdots k) \cdots (j \cdots k - 1), (j \dot{+} 1 \cdots j \dot{+} k) \cdots (n \cdots j + k - 1) \quad (5.3)$$

$$\bigcup_{k_1+k_2=k} (1 \cdots k_1 j \dot{+} 1 \cdots j \dot{+} k_2) \cdots \bigcup_{k_1+k_2=k} (j \cdots k_1 - 1 n \cdots j + k_2 - 1)\}.$$

The linear-dependencies of an on-shell diagram correspond to $k \times (n - k) - (2n - 4)$ minors m_i in \mathcal{M} vanishing. The set of these $k \times (n - k) - (2n - 4)$ minors is denoted as M_I . As conclusion, the on-shell bipartite diagram of the leading singularities of the loop amplitudes correspond to the Grassmannian cell $C^{k \times n}$ whose values can be completely fixed by the δ -function in (2.13) and the constraints $m_i = 0$ for arbitrary $m_i \in M_I$. In this way terms with the same Grassmannian geometry are collected together. We shall be using these properties in a crucial way to study the singularity structures of nonplanar NMHV amplitudes in this section. We shall as before use a specific example, in this case a 6-point NMHV nonplanar amplitude, to assist a general discussion whenever appropriate.

For the on-shell diagrams with same linear-structures characterized by M_I , we define a function

$$F_{M_I}^g = \oint_{C \in \bar{G}_{m_i=0, \forall m_i \in M_I}} \frac{d^{k \times n} C}{\text{vol}(GL(3)) \mathcal{P}_g} \frac{1}{\mathcal{P}_g} \delta^{k \times 4}(C \cdot \tilde{\eta}) \delta^{k \times 2}(C \cdot \tilde{\lambda}) \delta^{2 \times k}(\lambda \cdot C^\perp). \quad (5.4)$$

where $\bar{G}_{m_i=0}$ is a subset in $G(k, n)$ with $m_i = 0$, and $\oint_{C \in \bar{G}_{m_i=0}}$ picks up the residue on one minor $m_i = 0$ upon an integration along the contour, C in $\bar{G}_{m_i=0}$. In order to form an invariant top form and to include all existent poles, $\mathcal{P}_g \equiv \prod_{i=1}^n m_{g_i}$ and \mathcal{P}_g should scale uniformly as $\mathcal{P}_g(tC) = t^{k \times n} \mathcal{P}_g(C)$ and contain all the factors $m_i \in M_I$.

We therefore propose a general formula for nonplanar one-loop diagram in the invariant top form

$$\mathcal{A}_n^k(1 \cdots j, j \dot{+} 1 \cdots \dot{n}) = \sum_{M_I \subset \mathcal{M}} \mathcal{F}_{M_I}(1 \cdots j, j \dot{+} 1 \cdots \dot{n}), \quad (5.5)$$

where $\mathcal{F}_{M_I}(1 \cdots j, j \dot{+} 1 \cdots \dot{n}) \equiv \sum_g N_g F_{M_I}^g$. The sum runs over all the top forms with poles on the hypersurfaces, defined by $m_i = 0$, in $G(k, n)$. The coefficients, N_g , do not depend on C .

We consider a 6-point one-loop amplitude $\mathcal{A}(1, 2, 3, 4, 5, \dot{6})$ with “6” being the nonplanar leg. More general one-loop amplitudes and higher-loop amplitudes will be left to a future publication. The set of minors is

$$\mathcal{M} = \{(123), (234), (345), (451), (512), (612), (623), (634), (645), (651)\}. \quad (5.6)$$

with M_I containing only one element in \mathcal{M} . Then

$$F_{M_I}^j = \oint_{C \in \bar{G}_{m_i=0, \forall m_i \in M_I}} \frac{d^{3 \times 6} C}{\text{vol}(GL(3)) \mathcal{P}_j} \frac{1}{\mathcal{P}_j} \delta^{3 \times 4}(C \cdot \tilde{\eta}) \delta^{3 \times 2}(C \cdot \tilde{\lambda}) \delta^{2 \times 3}(\lambda \cdot C^\perp), \quad (5.7)$$

All possible products of minors are listed,

$$\left\{ \begin{array}{ll} \mathcal{P}_1 = (123)(234)(345)(645)(651)(612) & \mathcal{P}_6 = (123)(234)(451)(623)(645)(651) \\ \mathcal{P}_2 = (234)(345)(451)(623)(651)(612) & \mathcal{P}_7 = (234)(345)(512)(634)(651)(612) \\ \mathcal{P}_3 = (345)(451)(512)(623)(612)(634) & \mathcal{P}_8 = (345)(451)(123)(645)(623)(612) \\ \mathcal{P}_4 = (451)(512)(123)(623)(645)(634) & \mathcal{P}_9 = (451)(512)(234)(651)(623)(634) \\ \mathcal{P}_5 = (512)(123)(234)(645)(651)(634) & \mathcal{P}_{10} = (512)(123)(345)(612)(645)(634). \end{array} \right. \quad (5.8)$$

We need to verify that the amplitude is in the form

$$\mathcal{A}(12345\dot{6}) = \sum_{m_i \in \mathcal{M}} \mathcal{F}_{M_I}(12345\dot{6}) \equiv \sum_{M_I \in \mathcal{M}} \sum_j^{10} N_j F_{M_I}^j. \quad (5.9)$$

And we also need to determine the N_j . To this end we classify all the leading singularities into three type:

Type I: The nonplanar leg belongs to a 3-point amplitude after a double unitarity cut, as shown in Fig. 24, which are the same as a planar diagram up to a minus sign.

Type II: The nonplanar leg belongs to a 4-point amplitude after a double unitarity cut, as shown in Fig. 25, which can be transformed into a planar diagram up to a kinematic factor.

Type III: The nonplanar leg lies in a 5-point amplitude after a double unitarity cut, as shown in Fig. 26, which can also be transformed into a planar diagram up to an overall coefficient.

These three types of singularities are presented in Figs. 24, Fig. 25, and Fig. 26, respectively.

To arrive at the top form (5.9) we need to group terms with the same vanishing minor together. For example, if we consider $(123) = 0$, then according to Fig. 24, Fig. 25, and Fig. 26, we get

$$\mathcal{F}_{(123)}(12345|6) = \left\{ \begin{array}{ll} -(\mathcal{I}_{\{1,23,45,6\}} + \mathcal{I}_{\{5,6,123,4\}}) \mathcal{T}_{\{123456\}}^{(123)=0} - \mathcal{I}_{\{6,5,123,4\}} \mathcal{T}_{\{123465\}}^{(123)=0} & \text{Type I} \\ -(\mathcal{I}_{\{3,6,45,12\}} + \mathcal{I}_{\{4,5,123,6\}}) \mathcal{T}_{\{123645\}}^{(123)=0} & \text{Type II} \\ + \frac{s_{56}}{s_{5I_1}} \mathcal{I}_{\{3,4,56,12\}} \mathcal{T}_{\{123456\}}^{(123)=0} + \frac{s_{46}}{s_{4I_2}} \mathcal{I}_{\{1,23,46,5\}} \mathcal{T}_{\{123465\}}^{(123)=0} & \\ + \frac{s_{56}}{s_{5I_3}} \mathcal{I}_{\{2,3,456,1\}} \mathcal{T}_{\{123456\}}^{(123)=0} & \text{Type III,} \end{array} \right. \quad (5.10)$$

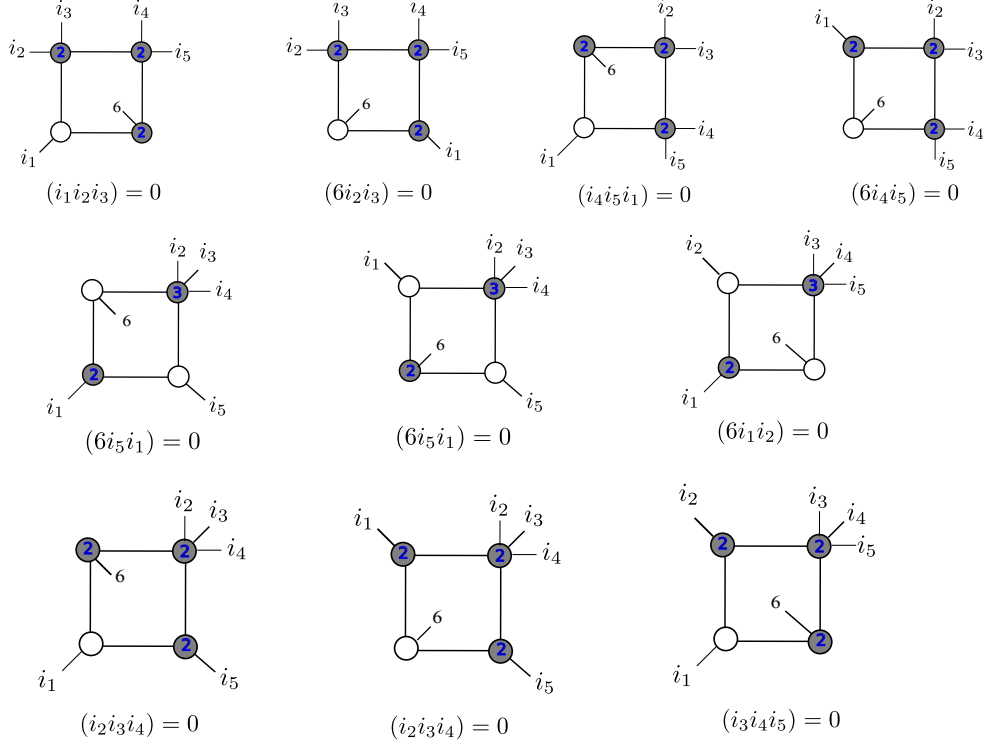


Figure 24. Leading singularity Type I

where

$$\begin{aligned}
 p_{I_1} &= \frac{(p_1 + p_2 + p_3)|\lambda_3\rangle \otimes [\tilde{\lambda}_4|(p_1 + p_2 + p_3)}{[\tilde{\lambda}_4|(p_1 + p_2 + p_3)|\lambda_3]}, \\
 p_{I_2} &= \frac{(p_1 + p_2 + p_3)|\lambda_1\rangle \otimes [\tilde{\lambda}_5|(p_1 + p_2 + p_3)}{[\tilde{\lambda}_5|(p_1 + p_2 + p_3)|\lambda_1]}, \\
 p_{I_3} &= \frac{(p_1 + p_2)|\lambda_3\rangle \otimes [\tilde{\lambda}_2|(p_1 + p_2)}{[\tilde{\lambda}_2|(p_1 + p_2)|\lambda_3]}, \\
 p_{I_5} &= \frac{(p_4 + p_5)|\lambda_4\rangle \otimes \langle\lambda_1|(p_2 + p_3)(p_4 + p_5)}{\langle\lambda_1|(p_2 + p_3)(p_4 + p_5)|\lambda_4)}.
 \end{aligned}$$

Here $\mathcal{I}_{\{1,2,3,4,6,5\}}$ is the scalar integration

$$\mathcal{I}_{\{1,2,3,4,6,5\}} = \int \frac{(p_1 + p_2 + p_3)^2 (p_1 + p_4 + p_6)^2}{l^2 (l + p_1)^2 (l + p_1 + p_2 + p_3)^2 (l - p_5)^2} \quad (5.11)$$

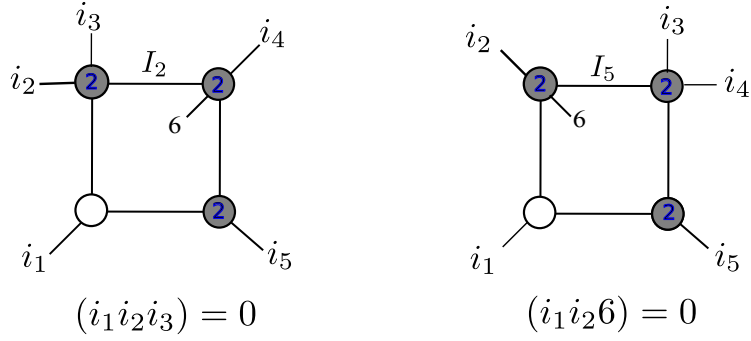
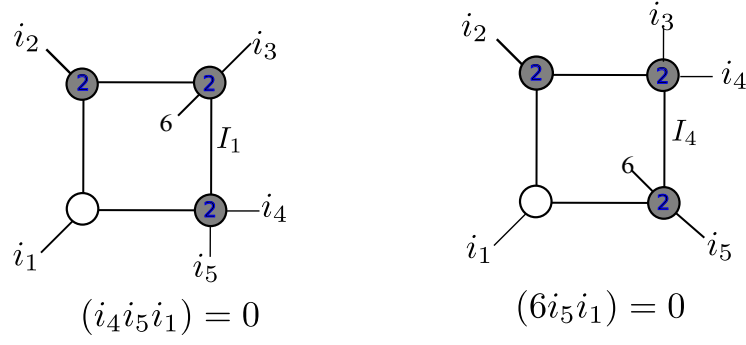


Figure 25. Leading singularity Type II

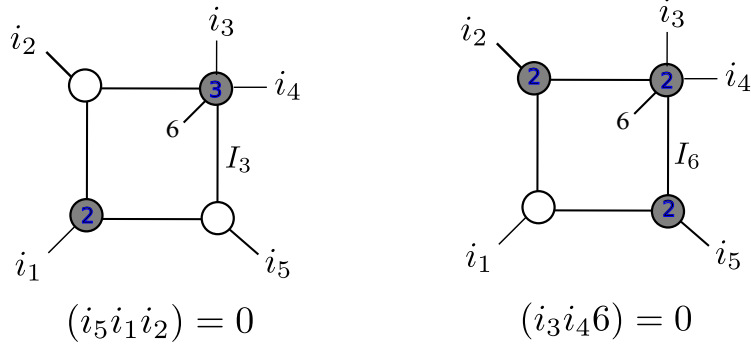


Figure 26. Leading singularity Type III

and $\mathcal{T}_{\{123645\}}^{(123)=0}$ is the cyclic integration around the pole $(123) = 0$ of the top-form [35] of the tree amplitudes with color ordering $\{123645\}$

$$\mathcal{T}_{\{123645\}}^{(123)=0} = \oint_{C \in \vec{G}_{(123)=0}} \frac{d^{3 \times 6} C}{\text{vol}(GL(3))} \frac{\delta^{3 \times 4}(C \cdot \tilde{\eta}) \delta^{3 \times 2}(C \cdot \tilde{\lambda}) \delta^{2 \times 3}(\lambda \cdot C^\perp)}{(123)(236)(364)(645)(451)(512)}, \quad (5.12)$$

and it works similarly for others. For Type II and Type III, the coefficients in (5.10)

are obtained by the permutation relation of a “box.” As it is explained in detail in Section 2.1, the permutation relation do not change the geometry of the Grassmannian cell.

Similarly, according to Fig. 24, Figs. 25, and Figs. 26, a sum of the terms with Grassmannian geometry $(612) = 0$ is

$$\mathcal{F}_{(612)}(12345\dot{6}) = \begin{cases} -(\mathcal{I}_{\{6,12,34,5\}} + \mathcal{I}_{\{1,2,345,6\}}) \mathcal{T}_{\{123456\}}^{(612)=0} - \mathcal{I}_{\{6,2,345,1\}} \mathcal{T}_{\{162345\}}^{(612)=0} & \text{Type I} \\ -(\mathcal{I}_{\{6,3,45,12\}} + \mathcal{I}_{\{6,345,1,2\}}) \mathcal{T}_{\{126345\}}^{(612)=0} & \text{Type II} \\ + \frac{s_{16}}{s_{1I_4}} \mathcal{I}_{\{2,3,45,61\}} \mathcal{T}_{\{123456\}}^{(612)=0} + \frac{s_{26}}{s_{2I_5}} \mathcal{I}_{\{1,26,34,5\}} \mathcal{T}_{\{126345\}}^{(612)=0} & \\ + \frac{s_{26}}{s_{2I_6}} \mathcal{I}_{\{4,5,126,3\}} \mathcal{T}_{\{126345\}}^{(612)=0} & \text{Type III,} \end{cases} \quad (5.13)$$

where

$$\begin{aligned} p_{I_4} &= \frac{(p_1 + p_2 + p_6)|\lambda_2\rangle \otimes [\tilde{\lambda}_3|(p_1 + p_2 + p_6)]}{[\tilde{\lambda}_3|(p_1 + p_2 + p_6)|\lambda_2]}, \\ p_{I_5} &= \frac{(p_1 + p_2 + p_6)|\lambda_1\rangle \otimes [\tilde{\lambda}_5|(p_1 + p_2 + p_6)]}{[\tilde{\lambda}_5|(p_1 + p_2 + p_6)|\lambda_1]}, \\ p_{I_6} &= \frac{(p_3 + p_4)|\lambda_4\rangle \otimes [\tilde{\lambda}_5|(p_3 + p_4)]}{[\tilde{\lambda}_5|(p_3 + p_4)|\lambda_4]}, \\ p_{\dot{2}} &= \frac{(p_1 + p_2)(p_4 + p_5)|\tilde{\lambda}_3\rangle \otimes [\tilde{\lambda}_1|(p_1 + p_2)]}{[\tilde{\lambda}_1|(p_1 + p_2)(p_4 + p_5)|\tilde{\lambda}_3]}. \end{aligned}$$

All other terms can be generated by cyclic permutations Z_5 of $\{12345\}$. And the total amplitude can be written as

$$\begin{aligned} \mathcal{A}(12345\dot{6}) &= \sum_{\sigma \in Z_5} \mathcal{F}_{(\sigma(1)\sigma(2)\sigma(3))}(\sigma(1)\sigma(2)\sigma(3)\sigma(4)\sigma(5)|6) \\ &\quad + \mathcal{F}_{(6\sigma(1)\sigma(2))}(\sigma(1)\sigma(2)\sigma(3)\sigma(4)\sigma(5)|6). \end{aligned} \quad (5.14)$$

The coefficients N_j are obtained by comparing (5.9), (5.10), (5.13) with (5.14). An interesting observation is that all the coefficients of the top-form for $\mathcal{P}_6 \cdots \mathcal{P}_{10}$ vanish, which, in turn, serves as a direct verification of our proposition (5.9).

6 Conclusion and Outlook

In this paper we present a new and useful permutation relation of Yangian Invariants. Different from KK and BCJ relations working at the level of amplitudes, it unveils a

relation between two Yangian Invariants with two consecutive legs exchanged. Interesting properties governing the permutations of Yangian Invariants can be uncovered in the bipartite on-shell diagram. For instance all Yangian Invariants have at least one “box” connecting to two external legs. When these two legs are exchanged the Grassmannian matrix does not change but maintain the same geometric property. The two Yangians are related by a simple kinematic factor which can be calculated recursively by BCFW method.

However, it is not always obvious to find the “box” due to the equivalence of bipartite on-shell diagrams. To this end we give a simple criterion from the associated permutation to check whether a given pair of consecutive legs are connected to a “box”. Because all consecutive legs in MHV amplitudes⁸ lie in a “box,” we can exchange any two legs at the expense of the kinematic factor. Most importantly, for a general diagram, if we exchange two lines—either internal or external—connecting to a “box” the geometry of the underlying Grassmannian will not be affected. This property can be interpreted as a new generator of equivalence in bipartite on-shell diagram—apart from square moves and mergers already observed in [35].

In the case of NMHV amplitudes there will be a special case—but only one case—that cannot be molded into a “box.” There arises a second basic building block in bipartite diagram, a “bridged twin-box” (Fig. 6), the permutation relation of which is discussed in Section 2.3. With these two permutation relations we can resolve all permutations in NMHV amplitudes in the process of constructing their total on-shell integrals.

In this paper we also present a systematic way to deal with the integrands of scattering amplitudes using unitarity cuts. Momentum twistor space is a natural language to reconstruct integrand without unphysical propagators. We discover a new way to add BCFW bridges and a new operation called “union” is introduced to combine results from different cuts to arrive at the total integrands. For one-loop planar MHV amplitudes our results coincide with those obtained from single cuts. The advantage of our proposal is its easy extension to NMHV and higher loops.

For nonplanar loop amplitudes we apply unitarity cuts to fix the loop momenta endowing them with a reasonable definition in the loop integrand. A crucial relation between planar and nonplanar elements has been discovered which, in turn, enable us to turn nonplanar components into planar ones at the expense of a simple kinematic factor. With on-shell diagrams we present detailed and systematic constructions of the total integrands for four- and five-point one-loop nonplanar MHV amplitudes. The

⁸MHV amplitudes have only one Yangian Invariant which is itself

kinematic factors as well as the corresponding planar amplitudes are separately dealt with using unitarity conditions. Final results are the “union” of all results reconstructed from all possible unitarity cuts.

Generalized unitarity cuts are used to address NMHV amplitudes. With six-point one-loop nonplanar as an explicit example, the amplitude after double unitarity cuts—with all loop momenta being fixed by the cut constraints—is a leading singularity without any variables. Interesting geometric properties, nevertheless, can be found in the non-planar leading singularities: it is the result of top-forms integrating around different poles.

There is an abundance of interesting open questions generated from these ideas. In the next paper we will present findings on the leading singularities in bipartite on-shell diagrams as well as a systematic way of building these diagrams in the twistor space. This way of dealing with leading singularities lends itself straightforward applications to higher loops. Furthermore, according to the geometric properties of the Yangian Invariants, say, collinearity or coplanarity of several points, we can further classify the permutation relations; and we will probably find permutation relations of non-adjacent legs. Moreover, interesting geometric shapes, such as knots, will appear in two loops. Ideas and methods in topology are called for to deal with higher-loop nonplanar amplitudes. Last but not the least we will apply our methodology to $\mathcal{N} < 4$ SYM or gauge theories in other dimensions.

Acknowledgments

Useful discussions with Nima Arkani-Hamed, Bo Feng, Yijian Du, Jens Fjelstad and Konstantin Savvidy are gratefully acknowledged. We would like to thank Ellis Yuan for proofreading the manuscript. Peizhi Du would like to thank Nima Arkani-Hamed for encouragement.

This research project has been supported in parts by the Jiangsu Ministry of Science and Technology under contract BK20131264 and by the Swedish Research Links programme of the Swedish Research Council (Vetenskapsradets generella villkor) under contract 348-2008-6049.

We also acknowledge 985 Grants from the Ministry of Education, and the Priority Academic Program Development for Jiangsu Higher Education Institutions (PAPD).

A The momentum twistor space

The introduction of momentum twistor space are discussed in [21, 22]. Here we summarize the basic concepts and some useful identities in momentum twistor space for completeness. In momentum space, the spinor form [55–59] of on-shell momentum is $p_{\alpha\dot{\alpha}} = p_\mu \sigma_{\alpha\dot{\alpha}}^\mu = \lambda_\alpha \tilde{\lambda}_{\dot{\alpha}}$, satisfying the constraint $p^2 = 0$ by construction. The momentum conservation, $\sum_{i=1}^n p_i = 0$, however, needs to be enforced by $\delta(\sum \lambda_i \tilde{\lambda}_i)$ in the scattering amplitudes. One often uses the dual coordinates x_i [60], where $p_i = x_i - x_{i-1}$, in which the momentum conservation $\sum_{i=1}^n p_i = 0$ is naturally satisfied, at the expense of $p_i^2 = 0$ being obscured. These two constraints are, however, both manifest in momentum twistor space, with twistor $Z = (\lambda, \mu)$ satisfying $\mu_{\dot{\alpha}} = x_{\alpha\dot{\alpha}} \lambda^\alpha$.

Any x_i in \mathbb{C}^4 corresponds to a projective line (Z_i, Z_{i+1}) in \mathbb{CP}^3 . Two lines (Z_{i-1}, Z_i) and (Z_i, Z_{i+1}) intersect at the point Z_i and the momentum $p^2 = (x_i - x_{i-1})^2 = 0$ is a null vector. When twistors are used to build momenta, the corresponding twistor space is called momentum twistor space [61, 62].

$\langle Z_i Z_j Z_k Z_l \rangle$ denotes the determinant of four twistors. If line $(Z_i Z_j)$ and $(Z_k Z_l)$ corresponds to the spacetime points x and y , the determinant is simply

$$\langle Z_i Z_j Z_k Z_l \rangle = \langle \lambda_i \lambda_j \rangle \langle \lambda_k \lambda_l \rangle (x - y)^2, \quad (\text{A.1})$$

where $\langle \lambda_i \lambda_j \rangle = \epsilon_{\alpha\beta} \lambda_i^\alpha \lambda_j^\beta$. In particular if two lines intersect, $(x - y)^2 = 0$, then the determinant vanishes. It implies that these four points are coplanar.

(abc) denotes the plane spanned by the three points Z_a, Z_b, Z_c , while $(ab) \cap (cde)$ denotes a point in twistor space where the line, (ab) , intersects with the plane, (cde) , and

$$(ab) \cap (cde) = Z_a \langle bcde \rangle + Z_b \langle cdea \rangle = -(Z_c \langle deab \rangle + Z_d \langle eabc \rangle + Z_e \langle abcd \rangle). \quad (\text{A.2})$$

With this definition we deduce that $(ab) \cap (cde) = -(cde) \cap (ab)$.

Likewise the line, $(abc) \cap (def)$, is the intersection of two planes (abc) and (def)

$$\begin{aligned} (abc) \cap (def) &= Z_a Z_b \langle cdef \rangle + Z_b Z_c \langle adef \rangle + Z_c Z_a \langle bdef \rangle \\ &= \langle abcd \rangle Z_e Z_f + \langle abcf \rangle Z_d Z_e + \langle abce \rangle Z_f Z_d. \end{aligned} \quad (\text{A.3})$$

Here we also give several very useful identities for momentum twistor space called *Schouten identity*. The familiar Schouten identity based on spinors is

$$\langle ac \rangle \langle bd \rangle = \langle ab \rangle \langle cd \rangle + \langle ad \rangle \langle bc \rangle. \quad (\text{A.4})$$

In momentum twistor space, any arbitrary set of five twistors $\{Z_a, Z_b, Z_c, Z_d, Z_e\}$ will satisfy the following identity,

$$Z_a\langle bcde \rangle + Z_b\langle cdea \rangle + Z_c\langle deab \rangle + Z_d\langle eabc \rangle + Z_e\langle abcd \rangle = 0. \quad (\text{A.5})$$

According to this, we could obtain the 5-term identity also called a Schouten identity:

$$\langle fg ha \rangle \langle bcde \rangle + \langle fg hb \rangle \langle cdea \rangle + \langle fg hc \rangle \langle deab \rangle + \langle fg hd \rangle \langle eabc \rangle + \langle fg he \rangle \langle abcd \rangle = 0. \quad (\text{A.6})$$

We will show another frequently used identity related to A and B, which is very analogous to (A.4),

$$\langle AB13 \rangle \langle AB24 \rangle = \langle AB12 \rangle \langle AB34 \rangle + \langle AB14 \rangle \langle AB23 \rangle. \quad (\text{A.7})$$

References

- [1] R. Britto, F. Cachazo, and B. Feng, *Computing one-loop amplitudes from the holomorphic anomaly of unitarity cuts*, *Phys. Rev. D* **71** (Jan., 2005) 025012, [[hep-th/0410179](#)].
- [2] R. Britto, F. Cachazo, and B. Feng, *New recursion relations for tree amplitudes of gluons*, *Nuclear Physics B* **715** (May, 2005) 499–522, [[hep-th/0412308](#)].
- [3] R. Britto, F. Cachazo, B. Feng, and E. Witten, *Direct Proof of the Tree-Level Scattering Amplitude Recursion Relation in Yang-Mills Theory*, *Physical Review Letters* **94** (May, 2005) 181602, [[hep-th/0501052](#)].
- [4] B. Feng and M. Luo, *An introduction to on-shell recursion relations*, *Frontiers of Physics* **7** (Oct., 2012) 533–575, [[arXiv:1111.5759](#)].
- [5] Z. Bern, L. Dixon, D. C. Dunbar, and D. A. Kosower, *One-loop n -point gauge theory amplitudes, unitarity and collinear limits*, *Nuclear Physics B* **425** (Aug., 1994) 217–260, [[hep-ph/9403226](#)].
- [6] Z. Bern, L. Dixon, D. C. Dunbar, and D. A. Kosower, *Fusing gauge theory tree amplitudes into loop amplitudes*, *Nuclear Physics B* **435** (Feb., 1995) 59–101, [[hep-ph/9409265](#)].
- [7] Z. Bern, L. J. Dixon, and V. A. Smirnov, *Iteration of planar amplitudes in maximally supersymmetric Yang-Mills theory at three loops and beyond*, *Phys. Rev. D* **72** (Oct., 2005) 085001, [[hep-th/0505205](#)].
- [8] R. Britto, F. Cachazo, and B. Feng, *Generalized unitarity and one-loop amplitudes in $N=4$ super-Yang Mills*, *Nuclear Physics B* **725** (Oct., 2005) 275–305, [[hep-th/0412103](#)].

- [9] R. Britto, E. Buchbinder, F. Cachazo, and B. Feng, *One-loop amplitudes of gluons in supersymmetric qcd*, *Phys. Rev. D* **72** (Sep, 2005) 065012.
- [10] E. I. Buchbinder and F. Cachazo, *Two-loop amplitudes of gluons and octa-cuts in Script $N = 4$ super Yang-Mills*, *Journal of High Energy Physics* **11** (Nov., 2005) 36, [[hep-th/0506126](#)].
- [11] H. van Deurzen, G. Luisoni, P. Mastrolia, E. Mirabella, G. Ossola, et al., *Multi-loop Integrand Reduction via Multivariate Polynomial Division*, [arXiv:1312.1627](#).
- [12] P. Mastrolia, E. Mirabella, G. Ossola, and T. Peraro, *Multiloop Integrand Reduction for Dimensionally Regulated Amplitudes*, [arXiv:1307.5832](#).
- [13] P. Mastrolia, E. Mirabella, G. Ossola, and T. Peraro, *Integrand-Reduction for Two-Loop Scattering Amplitudes through Multivariate Polynomial Division*, *Phys.Rev.* **D87** (2013) 085026, [[arXiv:1209.4319](#)].
- [14] P. Mastrolia, E. Mirabella, G. Ossola, T. Peraro, and H. van Deurzen, *The Integrand Reduction of One- and Two-Loop Scattering Amplitudes*, *PoS* **LL2012** (2012) 028, [[arXiv:1209.5678](#)].
- [15] Z. Bern, M. Czakon, D. Kosower, R. Roiban, and V. Smirnov, *Two-loop iteration of five-point $N=4$ super-Yang-Mills amplitudes*, *Phys.Rev.Lett.* **97** (2006) 181601, [[hep-th/0604074](#)].
- [16] J. J. Carrasco and H. Johansson, *Five-Point Amplitudes in $N=4$ Super-Yang-Mills Theory and $N=8$ Supergravity*, *Phys.Rev.* **D85** (2012) 025006, [[arXiv:1106.4711](#)].
- [17] Z. Bern, L. Dixon, D. Kosower, R. Roiban, M. Spradlin, et al., *The Two-Loop Six-Gluon MHV Amplitude in Maximally Supersymmetric Yang-Mills Theory*, *Phys.Rev.* **D78** (2008) 045007, [[arXiv:0803.1465](#)].
- [18] B. Eden, G. P. Korchemsky, and E. Sokatchev, *More on the duality correlators/amplitudes*, *Physics Letters B* **709** (Mar., 2012) 247–253, [[arXiv:1009.2488](#)].
- [19] B. Eden, P. Heslop, G. P. Korchemsky, and E. Sokatchev, *The super-correlator/super-amplitude duality: Part I*, *Nuclear Physics B* **869** (Apr., 2013) 329–377, [[arXiv:1103.3714](#)].
- [20] B. Eden, P. Heslop, G. P. Korchemsky, and E. Sokatchev, *The super-correlator/super-amplitude duality: Part II*, *Nuclear Physics B* **869** (Apr., 2013) 378–416, [[arXiv:1103.4353](#)].
- [21] N. Arkani-Hamed, J. Bourjaily, F. Cachazo, S. Caron-Huot, and J. Trnka, *The all-loop integrand for scattering amplitudes in planar $\mathcal{N} = 4$ SYM*, *Journal of High Energy Physics* **1** (Jan., 2011) 41, [[arXiv:1008.2958](#)].

- [22] N. Arkani-Hamed, J. Bourjaily, F. Cachazo, and J. Trnka, *Local integrals for planar scattering amplitudes*, *Journal of High Energy Physics* **6** (June, 2012) 125, [[arXiv:1012.6032](#)].
- [23] S. Caron-Huot and S. He, *Jumpstarting the all-loop S-matrix of planar $N = \{4\}$ super Yang-Mills*, *Journal of High Energy Physics* **7** (July, 2012) 174, [[arXiv:1112.1060](#)].
- [24] S. Caron-Huot, *Superconformal symmetry and two-loop amplitudes in planar $N = 4$ super Yang-Mills*, *Journal of High Energy Physics* **12** (Dec., 2011) 66, [[arXiv:1105.5606](#)].
- [25] L. F. Alday and J. Maldacena, *Gluon scattering amplitudes at strong coupling*, *Journal of High Energy Physics* **6** (June, 2007) 64, [[arXiv:0705.0303](#)].
- [26] L. F. Alday and J. Maldacena, *Comments on gluon scattering amplitudes via AdS/CFT*, *Journal of High Energy Physics* **11** (Nov., 2007) 68, [[arXiv:0710.1060](#)].
- [27] Z. Bern, J. J. M. Carrasco, and H. Johansson, *New relations for gauge-theory amplitudes*, *Phys. Rev. D* **78** (Oct., 2008) 085011, [[arXiv:0805.3993](#)].
- [28] R. Kleiss and H. Kuijf, *Multigluon cross sections and 5-jet production at hadron colliders*, *Nuclear Physics B* **312** (Jan., 1989) 616–644.
- [29] N. E. J. Bjerrum-Bohr, P. H. Damgaard, and P. Vanhove, *Minimal basis for gauge theory amplitudes*, *Phys. Rev. Lett.* **103** (Oct, 2009) 161602.
- [30] S. Stieberger, *Open & Closed vs. Pure Open String Disk Amplitudes*, [[arXiv:0907.2211](#)].
- [31] B. Feng, R. Huang, and Y. Jia, *Gauge Amplitude Identities by On-shell Recursion Relation in S-matrix Program*, *Phys.Lett.* **B695** (2011) 350–353, [[arXiv:1004.3417](#)].
- [32] S.-H. H. Tye and Y. Zhang, *Remarks on the identities of gluon tree amplitudes*, *Phys. Rev. D* **82** (Oct., 2010) 087702, [[arXiv:1007.0597](#)].
- [33] Y.-X. Chen, Y.-J. Du, and B. Feng, *A Proof of the Explicit Minimal-basis Expansion of Tree Amplitudes in Gauge Field Theory*, *Journal of High Energy Physics* **1102** (2011) 112, [[arXiv:1101.0009](#)].
- [34] F. Cachazo, *Fundamental BCJ Relation in $N=4$ SYM From The Connected Formulation*, *ArXiv e-prints* (June, 2012) [[arXiv:1206.5970](#)].
- [35] N. Arkani-Hamed, J. L. Bourjaily, F. Cachazo, A. B. Goncharov, A. Postnikov, et al., *Scattering Amplitudes and the Positive Grassmannian*, [[arXiv:1212.5605](#)].
- [36] S. Franco, D. Galloni, and A. Mariotti, *The Geometry of On-Shell Diagrams*, [[arXiv:1310.3820](#)].
- [37] M. Spradlin, A. Volovich, and C. Wen, *Three-Loop Leading Singularities and BDS Ansatz for Five Particles*, *Phys.Rev.* **D78** (2008) 085025, [[arXiv:0808.1054](#)].

- [38] F. Cachazo, M. Spradlin, and A. Volovich, *Leading Singularities of the Two-Loop Six-Particle MHV Amplitude*, *Phys.Rev.* **D78** (2008) 105022, [[arXiv:0805.4832](#)].
- [39] L. Dolan, C. R. Nappi, and E. Witten, *A Relation between approaches to integrability in superconformal Yang-Mills theory*, *JHEP* **0310** (2003) 017, [[hep-th/0308089](#)].
- [40] L. Dolan, C. R. Nappi, and E. Witten, *Yangian symmetry in $D = 4$ superconformal Yang-Mills theory*, [hep-th/0401243](#).
- [41] N. Arkani-Hamed, F. Cachazo, C. Cheung, and J. Kaplan, *The S -matrix in twistor space*, *Journal of High Energy Physics* **3** (Mar., 2010) 110, [[arXiv:0903.2110](#)].
- [42] N. Arkani-Hamed, F. Cachazo, C. Cheung, and J. Kaplan, *A duality for the S matrix*, *Journal of High Energy Physics* **3** (Mar., 2010) 20, [[arXiv:0907.5418](#)].
- [43] N. Arkani-Hamed, J. Bourjaily, F. Cachazo, and J. Trnka, *Unification of residues and Grassmannian dualities*, *Journal of High Energy Physics* **1** (Jan., 2011) 49, [[arXiv:0912.4912](#)].
- [44] R. G. Ambrosio, B. Eden, T. Goddard, P. Heslop, and C. Taylor, *Local integrands for the five-point amplitude in planar $N=4$ SYM up to five loops*, [arXiv:1312.1163](#).
- [45] Z. Bern, L. J. Dixon, D. Dunbar, M. Perelstein, and J. Rozowsky, *On the relationship between Yang-Mills theory and gravity and its implication for ultraviolet divergences*, *Nucl.Phys.* **B530** (1998) 401–456, [[hep-th/9802162](#)].
- [46] Z. Bern, J. Carrasco, L. J. Dixon, H. Johansson, and R. Roiban, *Manifest Ultraviolet Behavior for the Three-Loop Four-Point Amplitude of $N=8$ Supergravity*, *Phys.Rev.* **D78** (2008) 105019, [[arXiv:0808.4112](#)].
- [47] Z. Bern, J. Carrasco, L. J. Dixon, H. Johansson, and R. Roiban, *The Complete Four-Loop Four-Point Amplitude in $N=4$ Super-Yang-Mills Theory*, *Phys.Rev.* **D82** (2010) 125040, [[arXiv:1008.3327](#)].
- [48] Z. Bern, J. Carrasco, H. Johansson, and R. Roiban, *The Five-Loop Four-Point Amplitude of $N=4$ super-Yang-Mills Theory*, *Phys.Rev.Lett.* **109** (2012) 241602, [[arXiv:1207.6666](#)].
- [49] L. Bianchi and M. S. Bianchi, *Non-planarity through unitarity in ABJM*, [arXiv:1311.6464](#).
- [50] A. Ochirov, *All one-loop NMHV gluon amplitudes in $N=1$ SYM*, *JHEP* **1312** (2013) 080, [[arXiv:1311.1491](#)].
- [51] S. J. Parke and T. Taylor, *An Amplitude for n Gluon Scattering*, *Phys.Rev.Lett.* **56** (1986) 2459.
- [52] L. Dixon, *Calculating Scattering Amplitudes Efficiently*, *ArXiv High Energy Physics - Phenomenology e-prints* (Jan., 1996) [[hep-ph/96](#)].

- [53] A. Postnikov, *Total positivity, Grassmannians, and networks*, *ArXiv Mathematics e-prints* (Sept., 2006) [[math/0609](#)].
- [54] A. Knutson, T. Lam, and D. Speyer, *Positroid Varieties: Juggling and Geometry*, *ArXiv e-prints* (Nov., 2011) [[arXiv:1111.3660](#)].
- [55] F. A. Berends, R. Kleiss, P. De Causmaecker, R. Gastmans, W. Troost, et al., *Multiple Bremsstrahlung in Gauge Theories at High-Energies. 2. Single Bremsstrahlung*, *Nucl.Phys.* **B206** (1982) 61.
- [56] F. A. Berends, R. Kleiss, P. De Causmaecker, R. Gastmans, and T. T. Wu, *Single Bremsstrahlung Processes in Gauge Theories*, *Phys.Lett.* **B103** (1981) 124.
- [57] R. Kleiss and W. J. Stirling, *Spinor Techniques for Calculating p anti- $p \rightarrow W^{+-} / Z0 + Jets$* , *Nucl.Phys.* **B262** (1985) 235–262.
- [58] J. Gunion and Z. Kunszt, *Improved Analytic Techniques for Tree Graph Calculations and the $G g q$ anti- q Lepton anti-Lepton Subprocess*, *Phys.Lett.* **B161** (1985) 333.
- [59] Z. Xu, D.-H. Zhang, and L. Chang, *Helicity Amplitudes for Multiple Bremsstrahlung in Massless Nonabelian Gauge Theories*, *Nucl.Phys.* **B291** (1987) 392.
- [60] J. Drummond, J. Henn, V. Smirnov, and E. Sokatchev, *Magic identities for conformal four-point integrals*, *JHEP* **0701** (2007) 064, [[hep-th/0607160](#)].
- [61] R. Penrose, *Twistor algebra*, *J.Math.Phys.* **8** (1967) 345.
- [62] A. Hodges, *The Box Integrals in Momentum-Twistor Geometry*, *JHEP* **1308** (2013) 051, [[arXiv:1004.3323](#)].